# HHS Public Access

Author manuscript

*Acta Neuropathol.* Author manuscript; available in PMC 2018 May 01.

# Genome-wide association study identifies four novel loci associated with Alzheimer's endophenotypes and disease modifiers

**Yuetiva Deming**[1], **Zeran Li**[1], **Manav Kapoor**[2], **Oscar Harari**[1], **Jorge L. Del-Aguila**[1], **Kathleen Black**[1], **David Carrell**[1], **Yefei Cai**[1], **Maria Victoria Fernandez**[1], **John Budde**[1], **Shengmei Ma**[1], **Benjamin Saef**[1], **Bill Howells**[1], **Kuanlin Huang**[3,4], **Sarah Bertelsen**[2], **Anne M. Fagan**[5,6,7], **David M. Holtzman**[5,6,7,8], **John C. Morris**[5,6,7,8], **Sungeun Kim**[9,10], **Andrew J. Saykin**[9], **Philip L. De Jager**[11,12,13], **Marilyn Albert**[14], **Abhay Moghekar**[14], **Richard O'Brien**[15], **Matthias Riemenschneider**[16], **Ronald C. Petersen**[17], **Kaj Blennow**[18,19], **Henrik Zetterberg**[18,19,20], **Lennart Minthon**[21], **Vivianna M. Van Deerlin**[22], **Virginia Man-Yee Lee**[22], **Leslie M. Shaw**[22], **John Q. Trojanowski**[22], **Gerard Schellenberg**[22], **Jonathan L. Haines**[23], **Richard Mayeux**[24], **Margaret A. Pericak-Vance**[25], **Lindsay A. Farrer**[26], **Elaine R. Peskind**[27,28], **Ge Li**[27,29], **Antonio F. Di Narzo**[30], **Alzheimer's Disease Neuroimaging Initiative (ADGC). The Alzheimer Disease Genetic Consortium (ADGC)**, **John S. K. Kauwe**[31], **Alison M. Goate**[2], and **Carlos Cruchaga**[1,8]

[1]Department of Psychiatry, Washington University School of Medicine, 660 S. Euclid Ave. B8134, St. Louis, MO 63110, USA

[2]Department of Neuroscience, Ronald M Loeb Center for Alzheimer's Disease, Icahn School of Medicine at Mount Sinai, New York, NY, USA

[3]Department of Medicine, Washington University School of Medicine, 660 S. Euclid Ave. B8134, St. Louis, MO 63110, USA

[4]McDonnell Genome Institute, Washington University School of Medicine, 660 S. Euclid Ave. B8134, St. Louis, MO 63110, USA

[5]Department of Neurology, Washington University School of Medicine, 660 S. Euclid Ave., St. Louis, MO 63110, USA

[6]Knight Alzheimer's Disease Research Center, Washington University School of Medicine, 660 S. Euclid Ave., St. Louis, MO 63110, USA

[7]Hope Center for Neurological Disorders, Washington University School of Medicine, 660 S. Euclid Ave. B8111, St. Louis, MO 63110, USA

[8]Department of Developmental Biology, Washington University School of Medicine, 660 S. Euclid Ave., St. Louis, MO 63110, USA

[9]Indiana Alzheimer Disease Center and Center for Neuroimaging, Indiana University School of Medicine, Indianapolis, IN, USA

[10]Department of Electrical and Computer Engineering, State University of New York, Oswego, NY 13126, USA

[11]Program in Translational NeuroPsychiatric Genomics, Department of Neurology, Institute for the Neurosciences, Brigham and Women's Hospital, Boston, MA 02115, USA

[12]Harvard Medical School, Boston, MA 02115, USA

[13]Program in Medical and Population Genetics, Broad Institute of Harvard University and M.I.T., Cambridge, MA 02142, USA

[14]Department of Neurology, Johns Hopkins University School of Medicine, Baltimore, MD, USA

[15]Department of Neurology, Duke Medical Center, Box 2900, Durham, NC 27710, USA

[16]Clinic of Psychiatry and Psychotherapy, Saarland University, Homburg/Saar, Germany

[17]Department of Neurology, Mayo Clinic, Rochester, MN, USA

[18]Department of Psychiatry and Neurochemistry, Institute of Neuroscience and Physiology, The Sahlgrenska Academy at the University of Gothenburg, Mölndal, Sweden

[19]Clinical Neurochemistry Laboratory, Department of Neuroscience and Physiology, Sahlgrenska University Hospital, University of Gothenburg, Mölndal, Sweden

[20]Department of Molecular Neuroscience, UCL Institute of Neurology, Queen Square, London, UK

[21]Clinical Memory Research Unit, Department of Clinical Sciences, Lund University, Lund, Sweden

[22]Department of Pathology and Laboratory Medicine, Perelman School of Medicine at the University of Pennsylvania, Philadelphia, PA, USA

[23]Department of Molecular Physiology and Biophysics, Vanderbilt Center for Human Genetics Research, Vanderbilt University, Nashville, TN, USA

[24]Department of Neurology, Taub Institute on Alzheimer's Disease and the Aging Brain, and Gertrude H. Sergievsky Center, Columbia University, New York, NY, USA

[25]The John P. Hussman Institute for Human Genomics, and Dr. John T. Macdonald Foundation Department of Human Genetics, University of Miami, Miami, FL, USA

[26]Departments of Biostatistics, Medicine (Genetics Program), Ophthalmology, Epidemiology, and Neurology, Boston University, Boston, MA, USA

[27]Department of Psychiatry and Behavioral Sciences, University of Washington, Seattle, WA, USA

[28]VISN-20 Mental Illness Research, Education, and Clinical Center, VA Puget Sound Health Care System, Seattle, WA, USA

[29]VISN-20 Geriatric Research, Education, and Clinical Center, VA Puget Sound Health Care System, Seattle, WA, USA

[30]Department of Genetics and Genomic Sciences, Icahn School of Medicine at Mount Sinai, New York, NY, USA

[31]Department of Biology, Brigham Young University, Provo, UT, USA

## Abstract

More than 20 genetic loci have been associated with risk for Alzheimer's disease (AD), but reported genome-wide significant loci do not account for all the estimated heritability and provide little information about underlying biological mechanisms. Genetic studies using intermediate quantitative traits such as biomarkers, or endophenotypes, benefit from increased statistical power to identify variants that may not pass the stringent multiple test correction in case–control studies. Endophenotypes also contain additional information helpful for identifying variants and genes associated with other aspects of disease, such as rate of progression or onset, and provide context to interpret the results from genome-wide association studies (GWAS). We conducted GWAS of amyloid beta ($A\beta_{42}$), tau, and phosphorylated tau ($ptau_{181}$) levels in cerebrospinal fluid (CSF) from 3146 participants across nine studies to identify novel variants associated with AD. Five genome-wide significant loci (two novel) were associated with $ptau_{181}$, including loci that have also been associated with AD risk or brain-related phenotypes. Two novel loci associated with $A\beta_{42}$ near *GLIS1* on 1p32.3 ($\beta = -0.059$, $P = 2.08 \times 10^{-8}$) and within *SERPINB1* on 6p25 ($\beta = -0.025$, $P = 1.72 \times 10^{-8}$) were also associated with AD risk (*GLIS1*: OR = 1.105, $P = 3.43 \times 10^{-2}$), disease progression (*GLIS1*: $\beta = 0.277$, $P = 1.92 \times 10^{-2}$), and age at onset (*SER-PINB1*: $\beta = 0.043$, $P = 4.62 \times 10^{-3}$). Bioinformatics indicate that the intronic *SERPINB1* variant (rs316341) affects expression of *SERPINB1* in various tissues, including the hippocampus, suggesting that *SERPINB1* influences AD through an $A\beta$-associated mechanism. Analyses of known AD risk loci suggest *CLU* and *FERMT2* may influence CSF $A\beta_{42}$ ($P = 0.001$ and $P = 0.009$, respectively) and the *INPP5D* locus may affect $ptau_{181}$ levels ($P = 0.009$); larger studies are necessary to verify these results. Together the findings from this study can be used to inform future AD studies.

### Keywords

## Introduction

More than five million Americans suffer with Alzheimer's disease (AD), the most common neurodegenerative disease leading to progressive cognitive decline, and this number continues to increase as there are currently no effective methods to treat or prevent disease. Several genome-wide association studies (GWAS) have identified at least 24 loci containing common variants associated with AD risk [37, 39, 48, 56]. AD is a complex disease that is highly heritable, with an estimated heritability as high as 79% in twin studies [31] and genetic variance analyses estimate >53% of the variance in AD status can be explained by common variants (minor allele frequency, MAF > 1%) [64]. Polygenic studies have illustrated the genetic complexity underlying AD; recent studies using polygenic risk scores (PRS) calculated by combining the small effects of independent SNPs associated with AD risk ($P < 0.5$) provided AD risk prediction accuracy, as measured by area under the receiver operating curve (AUC) > 0.74, which is near the maximum AUC (0.82) [22, 23]. These studies indicate many genetic loci combine to increase risk for AD, most of the genetic risk loci are tagged by common variants (MAF > 1%), and that these loci, individually, have small effects on disease. These findings reveal that most AD risk variants have not passed the strict significance threshold required for multiple-test correction in GWAS, even in large studies such as the landmark study by the International Genomics of Alzheimer's Project (IGAP), involving more than 74,000 total individuals, which identified 11 novel loci associated with AD risk [48]. It is also important to note that most AD susceptibility loci identified in these GWAS are gene-dense regions and many significantly associated SNPs are non-coding (intronic or intergenic), making it difficult to determine which genes are involved or how identified variants influence these genes. Studies integrating alternative phenotypes, gene expression, and other omics data are important for understanding the underlying biology of AD.

There is significant evidence that AD pathology is present several years before the onset of clinical symptoms [25, 26, 41, 55]. Consequently, AD case–control GWAS can be confounded by the presence of preclinical "controls". Case– control-based GWAS are also limited to identifying genetic associations for disease risk; results from these studies do not provide information about other aspects of disease such as age at onset (AAO) or disease progression, or information about underlying biological mechanisms involved in pathogenesis. Endophenotypes are quantitative traits strongly associated with disease that also share genetic architecture with disease; therefore, genetic studies of endophenotypes are a powerful approach to identify loci associated with complex traits without many of the limitations of case–control studies. Cerebrospinal fluid (CSF) amyloid-beta1–42 ($A\beta_{42}$) and phosphorylated tau ($ptau_{181}$) are well-established AD endophenotypes [7, 13–15]. CSF $ptau_{181}$ levels are elevated in AD cases and positively correlate with the number of neurofibrillary tangles, while CSF $A\beta_{42}$ levels are lower in cases and correlate negatively with plaque load [43, 59, 72]. Increased CSF $ptau_{181}$ is predictive for cognitive decline and progression from mild cognitive impairment to AD [2, 16]. Some genetic variants associated with AD also influence CSF levels of $ptau_{181}$, $A\beta_{42}$, or both [13, 44]. We previously performed GWAS of CSF tau, $ptau_{181}$, and $A\beta_{42}$ on 1269 participants (591 cases, 687 controls) and identified four genome-wide significant loci associated with tau and $ptau_{181}$,

including a novel locus that also associated with AD risk, tangle pathology, and cognitive decline [13]. This study has been expanded more than twofold to 3146 participants across nine cohorts with CSF and genome-wide genotype data (Table 1), providing additional power to identify more novel loci associated with $ptau_{181}$, $A\beta_{42}$, and AD.

## Methods

### Ethics statement

The Institutional Review Boards of all participating institutions approved the study and research was carried out in accordance with the approved protocols. Written informed consent was obtained from participants or their family members.

### Cohort descriptions

CSF tau, ptau, and $A\beta_{42}$ were measured in 3146 individuals from nine different studies. There were 805 individuals (29.34% cases) enrolled in studies at the Charles F. and Joanne Knight Alzheimer's Disease Research Center (Knight ADRC), 787 individuals (more than 71% cases) from Alzheimer's Disease Neuroimaging Initiative (ADNI; 390 from ADNI1 and 397 from ADNI2), 184 individuals (5.43% cases) from BIOCARD: Predictors of Cognitive Decline Among Normal Individuals (BIOCARD), 105 individuals (no AD status) from Saarland University in Homburg/Saar, Germany (HB), 433 individuals (22.17% cases) from Mayo Clinic (MAYO), 293 individuals (all cases) from Skåne University Hospital, Sweden (SWEDEN), 164 (62.8% cases) from studies at Perelman School of Medicine at the University of Pennsylvania (UPENN), and 375 (33.33% cases) from studies at the University of Washington (UW). Table 1 shows the demographic data for each study. Clinical assessments, CSF collection, and proteins were measured by each site. Clinical dementia rating (CDR) was available for 86% of the total data set. The CDR is a five-point scale used to describe the overall dementia severity for each individual (no dementia = 0, very mild = 0.5, mild = 1, moderate = 2, and severe = 3). Individuals with CDR = 0 were categorized as controls, cases were defined as individuals with CDR > 0.

### Genotyping and imputation

Samples were genotyped with the Illumina 610 or Omniexpress chip. Stringent quality control (QC) criteria were applied to each genotyping array separately before combining genotype data. The minimum call rate for single nucleotide polymorphisms (SNPs) and individuals was 98% and autosomal SNPs not in Hardy–Weinberg equilibrium ($P < 1 \times 10^{-6}$) were excluded. X-chromosome SNPs were analyzed to verify sex identification. Unanticipated duplicates and cryptic relatedness (Pihat  0.25) among samples were tested by pairwise genome-wide estimates of proportion identity-by-descent, and when a pair of identical or related samples was identified, the sample from Knight ADRC or with a higher number of variants that passed QC was prioritized. EIGENSTRAT [61] was used to calculate principal components. *APOE* ε2, ε3, and ε4 isoforms were determined by genotyping rs7412 and rs429358 using Taqman genotyping technology as previously described [14, 15, 44]. The 1000 Genomes Project Phase 3 data (October 2014), SHAPEIT v2.790 [18], and IMPUTE2 v2.3.2 [40] were used for phasing and imputation. Individual genotypes imputed with probability <0.90 were set to missing and imputed genotypes with

probability   0.90 were analyzed as fully observed. Genotyped and imputed variants with MAF < 0.02 or IMPUTE2 information score <0.30 were excluded, leaving 7,358,575 variants for analyses.

## Data normalization for statistical analyses

Prior to combining data for analyses, CSF levels of tau, ptau, and $A\beta_{42}$ were $\log_{10}$-transformed to approximate a normal distribution and the mean from each data set was standardized to zero to account for the different platforms used by different studies to measure protein levels. There were no significant differences in the transformed and standardized values for the different studies. Study, age, sex, and the first two principal components were identified as confounding factors by stepwise regression analyses for each protein and corrected for in applicable analyses.

## Experimental design and data modeling

Studies by our group, and others, have demonstrated that when there is GWAS data available for all samples, a one-stage GWAS of combined data from both stages of a two-stage GWAS provides more power to identify genetic association than analyzing the groups separately, despite the fact that the one-stage GWAS requires a more stringent threshold to determine significance [13–15, 19, 70]. To maximize the power in our analyses, we performed a one-stage joint-GWAS. The CSF levels were measured with different platforms and at different sites, consequently the raw values could not be combined. Instead, the raw values were $\log_{10}$-transformed to approximate a normal distribution within each separate study and centralized by each study mean. We have used this approach in previous studies and demonstrated that it is an effective way to correct for study differences [13, 19]. We also performed analyses to ensure the results were not confounded by any study bias; to determine if the top hits were being driven by any individual study, we analyzed each dataset separately and performed meta analyses. The directions of effect for the genome-wide significant signals for $A\beta_{42}$ and $ptau_{181}$ were consistent across studies when analyzed separately and results from meta-analyses of the individual studies were consistent with the joint results even after removing cohort from previous study (Supplementary Figs. 1–3).

## Alternative mixed model method to normalize $A\beta_{42}$

Since CSF levels of $A\beta_{42}$ are lower in AD cases than controls, begin decreasing prior to clinical symptom onset [25, 26, 43, 59, 72], and the studies in this dataset varied in proportion of cases to controls, we wondered if a mixture modeling approach would be more appropriate for standardizing the data between studies instead of centering on the mean of each study. This method was successfully used previously to classify AD cases in two independent cohorts with at least 94% sensitivity [17]. Mixture modeling is a statistical method for estimating subpopulations within an overall group; in this case we assumed two normally distributed subgroups within each dataset representing individuals with low $A\beta_{42}$, therefore likely to be AD cases or preclinical, and with high $A\beta_{42}$, likely to be cognitively normal controls. Using an expectation–maximization algorithm, we calculated estimated means, standard deviations, and subgroup proportions for each study. Based on the assumption of two univariate normal distributions within each study we obtained two estimated means ($\mu_1$ and $\mu_2$), two estimated standard deviations ($\sigma_1$ and $\sigma_2$), and two

estimated mixing proportions ($\lambda_1$ and $\lambda_2$). We used these results to calculate the intersection of the estimated Gaussian curves using the following formula (Eq. 1):

$$\frac{-\left(\frac{\mu_1}{\sigma_1^2} - \frac{\mu_2}{\sigma_2^2}\right) \pm \sqrt{\left(\frac{\mu_1}{\sigma_1^2} - \frac{\mu_2}{\sigma_2^2}\right)^2 - 4\left(\frac{1}{2}\left(\frac{1}{\sigma_2^2} - \frac{1}{\sigma_1^2}\right)\right)\left(\frac{1}{2}\left(\frac{\mu_2^2}{\sigma_2^2} - \frac{\mu_1^2}{\sigma_1^2}\right) - \log\left(\frac{\sigma_1}{\sigma_2} \times \frac{\lambda_2}{\lambda_1}\right)\right)}}{2\left(\frac{1}{2}\left(\frac{1}{\sigma_2^2} - \frac{1}{\sigma_1^2}\right)\right)},$$ (1)

analyte, including study, age, sex, and the first two principal components as covariates in the default model [11]. The genomic inflation factor was $\lambda = 1.02$ for $\text{ptau}_{181}$ and $\lambda = 1.03$ for tau and $A\beta_{42}$ (Supplementary Fig. 7). There were no novel genetic associations identified for CSF tau levels (Supplementary Fig. 8 and Supplementary Table 2) but we did identify novel associations for $\text{ptau}_{181}$ and $A\beta_{42}$ (Figs. 1, 2; Table 2; Supplementary Tables 3, 4). Conditional analyses were conducted to identify additional independent signals in a locus by adding the SNP with the smallest $P$ value as a covariate into the default regression model and testing all remaining regional SNPs for association (Supplementary Figs. 9, 10). AD status, CDR, *APOE* alleles, *APOE* ε4 carrier status, $A\beta_{42}$, or $\text{ptau}_{181}$ levels were corrected for in additional analyses to determine the effects of these phenotypes on the genetic associations (Supplementary Fig. 11 and Supplementary Table 5–Supplementary Table 8). The combined dataset was stratified by AD status and cases and then centered the $\log_{10}$-transformed $A\beta_{42}$ levels to the intersection of the curves instead of the means for each study (Supplementary Table 1). CSF $A\beta_{42}$ thresholds have been determined previously for both ADNI (192 pg/mL) [69] and ADRC (500 pg/mL) [25]; the calculated intersects were comparable to these values (182 and 548 pg/mL, respectively, Supplementary Table 1). The density plots of the estimated subpopulations for each study ft the overall distributions reasonably well, but after accounting for AD status the model did not appear significantly different than standardizing to the overall mean (Supplementary Figs. 4, 5). There was no difference between the two methods in a single variant analysis of the mixed model standardized CSF $A\beta_{42}$ levels and the levels centered at the study mean (Supplementary Fig. 6).

The intersect was $\log_{10}$-transformed and subtracted from the $\log_{10}$-transformed values of $A\beta_{42}$ (Supplementary Figs. 4, 5 and Supplementary Table 1). When the singlevariant analysis was repeated using these normalized values for $A\beta_{42}$, the results were comparable to those from the mean normalized values (Supplementary Fig. 6). Therefore, to be consistent, we used the mean normalized values in all analyses.

### Association testing

The additive linear regression model in PLINK v1.9 [11] was used for single-variant analyses for each controls were analyzed separately for single-variant associations (Supplementary Table 8). Statistical significance for the single-variant analyses was based on the commonly used threshold from Bonferroni correction of the likely number of independent tests in genome-wide analyses ($P < 5 \times 10^{-8}$). Manhattan plots and regional association plots were created using the R package qqman v0.1.2 [74] and LocusZoom v1.3 [62], respectively.

### Meta-analyses

To test for potential systematic differences between the datasets, each study was analyzed separately for the most significant SNPs from the joint analyses. Covariates were age, sex, and the first two principal components. Meta-analyses of the results from the separate datasets were performed using METAL (version released 2011-03–25) [80]. The METAL default analysis scheme was used with sample size and beta for each SNP taken into account when combining $P$ values across studies. For the genome-wide significant signals, the nine studies showed consistent direction of effect individually, and meta-analysis results were consistent with the joint results (Supplementary Figs. 1, 2). After removing the samples that comprised the previously published study [13], the meta-analysis results remained consistent with the joint results (Supplementary Fig. 3). Forest plots were generated using the R package rmeta v2.16.

### Association with AD risk, progression, AAO

Results from independent analyses of different cohorts for AD risk [48], AAO (personal communication: Huang & Goate), and disease progression were analyzed to determine whether loci associated with CSF tau, ptau$_{181}$, and A$\beta_{42}$ were also associated with other AD phenotypes. Results for the most significantly associated SNPs for CSF tau, ptau$_{181}$, and A$\beta_{42}$ are reported here from the largest previously published two-stage meta-analysis of GWAS for AD risk consisting of a total 25,580 cases and 48,466 controls [48], and a recently published genome-wide survival analysis of AAO consisting of 39,855 individuals (personal communication: Huang & Goate). To determine disease progression in an independent cohort of 1530 individuals, we utilized the CDR Sum of Boxes (CDR-SB) which has been demonstrated to accurately stage dementia severity [57, 58]. Overall CDR is derived from scores in six individual categories (boxes) of memory, orientation, problem solving, community involvement, involvement in home and hobbies, and personal care; CDR-SB is a sum of the six boxes which provides a semi-continuous measure of symptomatic AD dementia from 0 (cognitively normal) to 18 (the most severe dementia). Disease progression from longitudinal studies at ADNI ($n = 728$) and Knight ADRC ($n = 802$) was modeled as the change in CDR-SB per year, adjusting for age, sex, baseline CDR, follow-up time, level of education, site, and PCs (Supplementary Table 9). Samples with 3 clinical assessments over 1.5 years after being diagnosed with AD were selected for the analysis and a mixed-model repeated measure framework was used to account for correlation between repeated measures in the same individual. We selected the appropriate optimal variance–covariance structure that minimizes the Akaike Information Criterion for testing the null model AR1 [14].

### Functional annotation

All SNPs below the suggestive significance threshold ($P = 1 \times 10^{-5}$) were taken forward for functional annotation using ANNOVAR version 2015-06–17 [77] and examined for potential regulatory functions using RegulomeDB v1.1 [8] and HaploReg v4.1 [78]. The search tools on the Genotype-Tissue Expression (GTEx) Analysis Release V6, dbGaP Accession phs000424.v6.p1 portal [33], data from the Brain eQTL Almanac (Braineac) [73] analyzed with the R package MatrixEQTL [68], and the Blood eQTL browser [79] were utilized to

determine if genome-wide significant SNPs were reported eQTLs. The Brain RNA-Seq database (http://web.stanford.edu/group/barres_lab/brainseqMariko/brainseq2.html) was mined to determine if genes of interest were expressed in the brain and in which cell types [84].

### Summary data-based mendelian randomization

To prioritize the putative causal variant from the ptau$_{181}$ and A$\beta_{42}$ associated variants, we used the Summary data-based Mendelian Randomization (SMR) method which tests the functional association between gene expression levels (measured by probes) and a trait (such as CSF protein levels) through the regression of estimated effect sizes [85]. Based on the assumptions of Mendelian randomization, any gene–trait association identified in this analysis should be free of confounding from non-genetic factors. To distinguish causality of a single variant on both gene expression and the trait vs linkage of two distinct genetic variants in LD with one affecting expression and one affecting the trait, the SMR method uses a heterogeneity (HEIDI) test. For the SMR analysis, we utilized the estimates of SNP effects on gene expression from summary data of a large-scale eQTL study with gene expression measured in peripheral blood (Blood eQTL browser) [79] and gene expression data from Cardiogenics measured in macrophages [35]. There were 3000 SNPs present in both the blood eQTL data and the GWAS results so the statistical significance threshold was defined (based on Bonferroni correction) as $P < 1.67 \times 10^{-5}$ for the associations between eQTL in blood and CSF GWAS loci. Focusing on the *SERPINB1* gene region (from the 6p terminal to 10 Mb after the defined *SERPINB1* transcription region) in the macrophage eQTL data, there were 4336 SNPs; therefore, the statistical significance threshold was defined as $P < 1.15 \times 10^{-5}$. The HEIDI threshold was set at $P > 0.05$ to be conservative; since the null hypothesis is that there is only one causal variant, a $P > 0.05$ indicates the variant that passed the SMR test is the causal variant.

### Genetic variance estimation

The Genome-wide Complex Trait Analysis (GCTA) v1.25.2 tool [82] was used to estimate the proportion of phenotypic variance explained by the common (MAF > 0.02) imputed and genotyped autosomal variants. The restricted maximum likelihood (REML) analysis was performed on the log$_{10}$-transformed standardized analyte values adjusted for age and gender with the first two principal components as covariates. Results are reported in Supplementary Table 10.

Since it was reported that estimated $h^2$ may be biased if causal variants are enriched in areas with lower or higher LD than average [81], we also used GCTA to calculate segment-based LD scores (segment length = 200 kb) for all SNPs in the REML analysis and plotted the number of SNPs from the single-variant analyses of A$\beta_{42}$ and ptau$_{181}$ with $P < 1 \times 10^{-5}$ (Supplementary Fig. 12). Since the most significantly associated SNPs showed LD heterogeneity, and the method can be applied to imputed GWAS data, we used the LD- and MAF-stratified genomic-REML (GREML-LDMS) method [81] in GCTA to estimate $h^2$ for each LD quartile and calculate a total $h^2$ estimate (Supplementary Table 10). The GCTA-GREML power calculator (http://cnsgenomics.com/shiny/gctaPower) [76] was used to calculate the power of the REML and GREML-LDMS analyses with the actual sample sizes,

estimated $h^2$, $\alpha = 0.05$, and genetic variance $= 2 \times 10^{-5}$ as parameters (Supplementary Table 10).

### Polygenic risk score

PRS were calculated using a weighted sum of the AD risk alleles reported by IGAP [48]. Weights for SNPs outside the *APOE* region were calculated by transforming the reported odds ratios by a base-2 logarithm. Proxy SNPs were utilized if the reported SNPs were unavailable in our data or did not pass QC; proxies were selected with the highest $R^2$ and D' values to the reported IGAP SNP in our genetic data and in 1000 Genomes. Since *APOE* has a large effect on AD risk and CSF protein levels, we calculated a default PRS without *APOE*. The effects of *APOE* genotype on AD risk are not additive, so *APOE* genotypes were weighted by the effects reported previously for each genotype ($\varepsilon2/\varepsilon2$ OR = 0.6, $\varepsilon2/\varepsilon3$ OR = 0.6, $\varepsilon2/\varepsilon4$ OR = 2.6, $\varepsilon3/\varepsilon4$ OR = 3.2, $\varepsilon4/\varepsilon4$ OR = 14.9) [29]. The SNPs that composed the PRS are listed in Supplementary Table 11. The PRS were calculated (with and without *APOE* genotype) using the score function in PLINK v1.90b3.42 [11], including the no-mean-imputation option to ensure scores would not be imputed for missing genetic data. The resulting mean score per allele was multiplied by the allele count to generate a total PRS.

## Results

### Reproduction of previously reported associations with CSF Aβ$_{42}$, tau, and ptau$_{181}$

As reported previously, the most significant variant associated with CSF levels of Aβ$_{42}$, tau, and ptau$_{181}$ was a proxy SNP for *APOE* $\varepsilon$4 ($r^2 = 0.726$, D' $= 1$), rs769449[A] (Aβ$_{42}$ $\beta = -0.117$, $P = 9.02 \times 10^{-47}$; tau $\beta = 0.082$, $P = 1.95 \times 10^{-16}$; ptau$_{181}$ $\beta = 0.091$, $P = 2.56 \times 10^{-18}$) [13]. In the current analyses, the effects were similar to what was previously reported with more significant $P$ values due to the larger sample size (Aβ$_{42}$ $\beta = -0.101$, $P = 4.78 \times 10^{-94}$; tau $\beta = 0.078$, $P = 4.05 \times 10^{-29}$; ptau$_{181}$ $\beta = 0.081$, $P = 9.51 \times 10^{-35}$). While there were no other loci associated with Aβ$_{42}$ in the previous GWAS, two loci outside the *APOE* locus were identified to be associated with CSF tau and ptau$_{181}$ [13]. We also replicated the previously reported loci for ptau$_{181}$ on 3q28 (rs9877502[A] near *GMNC*, $\beta = 0.044$, $P = 1.68 \times 10^{-7}$) and on 9p24.2 (rs514716[C] on *GLIS3*, $\beta = -0.072$, $P = 3.22 \times 10^{-9}$) were both genome-wide significant in this larger study (rs9877502[A], $\beta = 0.032$, $P = 6.35 \times 10^{-9}$; rs514716[C], $\beta = -0.049$, $P = 2.94 \times 10^{-8}$) (Table 2, Supplementary Fig. 13; see Supplementary Table 4 for all loci with $P < 1 \times 10^{-5}$) [13].

A small GWAS of AD CSF biomarkers from 374 ADNI participants (102 controls) identified variants in *EPC2* associated with CSF levels of tau and the Tau/Aβ$_{42}$ ratio [46]. In our current analyses, there were no genome-wide significant, or suggestive, associations with the *EPC2* locus (tau: $\beta = 0.005$, $P = 0.428$; Tau/Aβ$_{42}$ ratio $\beta = 0.072$, $P = 0.017$), but interestingly the strongest association was for Aβ$_{42}$ ($\beta = -0.016$, $P = 3.77 \times 10^{-4}$; Supplementary Fig. 14). Another early GWAS of CSF levels from 410 ADNI participants (119 controls) did not identify any genome-wide significant variants for CSF Aβ$_{42}$, ptau$_{181}$, or tau in cases, but found three genome-wide significant signals for Aβ$_{42}$ in controls (*CYP19A1, NCAM2*, and *ARL5B*) [36]; none of these loci were associated with Aβ$_{42}$ in

our current analyses of the joint dataset, cases-only, or controls-only ($P > 0.1$). A recent GWAS with only AD cases ($N = 363$) reported that SNPs located in the *SUCLG2* region were associated with CSF A$\beta_{42}$ levels [63] but this region was not associated with A$\beta_{42}$ in any of the current analyses of the joint dataset, cases-only, or controls-only ($P > 0.1$). *FRA10AC1* variants were associated with CSF A$\beta_{42}$ levels in a two-stage GWAS of data from ADNI (two discovery sets: $N = 391$ and $N = 385$; replication set $N = 204$), and although there were no genome-wide significant signals within the *FRA10AC1* locus in the current analyses, there was a near suggestive association between A$\beta_{42}$ and indel rs143151810[-] ($\beta = -0.033$, $P = 8.13 \times 10^{-5}$; Supplementary Fig. 14), which is in high LD with the SNP identified in the other study, rs10509663[G] ($r^2 = 0.987$, $D' = 0.997$), and both associations showed the same direction of effect on A$\beta_{42}$ levels [51].

### *APOE* locus significantly influences CSF levels of ptau$_{181}$ and tau independently of A$\beta_{42}$

As we reported previously, the *APOE* region was still significantly associated with ptau$_{181}$ after including CSF A$\beta_{42}$ levels in the analysis (rs769449[A]: default, $\beta$SNP = 0.079, $P = 5.30 \times 10^{-33}$; adjusted for A$\beta_{42}$ levels, $\beta_{SNP} = 0.046$, $P = 2.08 \times 10^{-11}$), and in the current analysis the association between rs769449[A] and ptau$_{181}$ remained genome-wide significant after including the interaction between A$\beta_{42}$ levels and *APOE* genotype in the model ($\beta_{SNP} = 0.042$, $P = 1.65 \times 10^{-8}$), suggesting *APOE* may influence tau pathology independently of A$\beta_{42}$ and supporting our previous findings (Supplementary Fig. 11 and Supplementary Table 5) [13]. Similar results were observed with CSF tau as well (default, $\beta_{SNP} = 0.077$, $P = 6.75 \times 10^{-28}$; adjusted for A$\beta_{42}$ levels, $\beta_{SNP} = 0.048$, $P = 4.11 \times 10^{-11}$; A$\beta_{42}$ and *APOE* genotype interaction, $\beta_{SNP} = 0.045$, $P = 1.04 \times 10^{-8}$). Low A$\beta_{42}$ levels (ADRC < 500 pg/mL and ADNI < 192 pg/ mL) have been associated with amyloid positron emission tomography (PET-PIB) evidence of A$\beta$ deposition [25, 69]. To determine if the possible presence of A$\beta$ pathology influenced the effect of the *APOE* locus on ptau$_{181}$ levels as we reported previously [13], we stratified the data from ADRC, ADNI1, and ADNI2 by high and low levels of A$\beta_{42}$ and found the association between *APOE* locus and ptau$_{181}$ levels in both groups with a higher effect size in the individuals with low A$\beta_{42}$ ($\beta = 0.055$, $P = 2.12 \times 10^{-7}$) than those with high A$\beta_{42}$ ($\beta = 0.037$, $P = 1.05 \times 10^{-2}$).

We wanted to determine if the signal in the *APOE* locus was driven entirely by *APOE* genotype (*APOE* ε2, ε3, and ε4), or if there was an independent signal influencing CSF levels of ptau$_{181}$ and A$\beta_{42}$, so we performed conditional analyses on *APOE* genotype accounting for both ε 2 and ε 4 effects. The *APOE* genotype showed the strongest association with CSF levels of ptau$_{181}$ ($\beta = 0.042$, $P = 3.13 \times 10^{-40}$) and A$\beta_{42}$ ($\beta = -0.053$, $P = 8.88 \times 10^{-114}$) after correcting for age, sex, study, and two principal components. The association between the top hit in the *APOE* locus (rs769449) and ptau$_{181}$ or A$\beta_{42}$, remained significant, but not genome-wide significant, after adding *APOE* genotype to the model (ptau$_{181}$: $\beta = 0.034$, $P = 1.07 \times 10^{-3}$; A$\beta_{42}$: $\beta = -0.036$, $P = 1.65 \times 10^{-6}$) suggesting that there may be a signal in this region independent of *APOE* ε2, ε3, and ε 4 (Supplementary Table 12). To further explore this finding, we conditioned on the most significant SNP (rs769449), which is in high LD for the *APOE* ε 4 allele (rs429358[C], $D' = 1$, $r^2 = 0.726$). We found that although the associations between *APOE* genotype and ptau$_{181}$ and A$\beta_{42}$ decreased, they remained genome-wide significant (conditioned: $\beta = 0.029$, $P = 5.91 \times 10^{-9}$

and $\beta = -0.040$, $P = 2.28 \times 10^{-28}$, respectively) (Supplementary Table 12). Together, these results suggest that most of the signal in this region is driven by *APOE* genotype, but additional independent SNPs in this region may influence CSF levels of both ptau$_{181}$ and A$\beta_{42}$.

### Novel associations in single-variant regression analyses for A$\beta_{42}$ and ptau$_{181}$

The genomic inflation was minimal in all analyses suggesting no evidence of confounding by systematic biases (default model $\lambda = 1.03$ for A$\beta_{42}$ and tau, 1.02 for ptau$_{181}$; Supplementary Fig. 7). In addition to the loci reported previously, two novel genetic associations with CSF ptau$_{181}$ were identified on 13q21.1 (rs9527039[C] near *PCDH8*, $\beta = -0.061$, $P = 5.95 \times 10^{-9}$) and 18q23 (rs12961169[T] near *CTDP1*, $\beta = 0.050$, $P = 5.12 \times 10^{-10}$) (Fig. 1; Table 2). We also identified, for the first time, two genome-wide significant loci outside of the *APOE* region associated with CSF A$\beta_{42}$ on 1p32.3 (rs185031519[G] near *GLIS1*, $\beta = -0.059$, $P = 2.08 \times 10^{-8}$) and on 6p25 (rs316341[G] within *SER-PINB1*, $\beta = -0.025$, $P = 1.72 \times 10^{-8}$) (Fig. 2; Table 2; see Supplementary Table 3 for all loci with $P < 1 \times 10^{-5}$). Conditioning on the most significant SNPs in each of these identified loci did not reveal any additional genome-wide significant signals (Supplementary Figs. 9, 10).

When clinical dementia rating (CDR) or clinical status were included in the model for either A$\beta_{42}$ or ptau$_{181}$, the results for the top loci were not significantly different than the default model (Supplementary Table 7), and when the analyses were stratified by AD status, the betas were similar for cases and controls (Supplementary Table 8). When individuals were stratified by high or low CSF A$\beta_{42}$ levels (A$\beta_{42}$ threshold: ADRC = 500 pg/ mL [25], ADNI = 192 pg/mL [69]), the betas for the top loci were similar between the two groups (Supplementary Table 8). These results suggest that all of the individuals in this study contributed to the associations with CSF A$\beta_{42}$ and ptau$_{181}$ levels, independent of status or amyloid pathology.

### Effects of associated genetic loci on other AD phenotypes

Since the purpose of studying these AD endophenotypes was to identify genetic factors associated with AD, we tested the genome-wide significant loci for associations with AD risk [48], rate of AD progression [58], or AAO (personal communication: Huang & Goate) in independent cohorts. The loci associated with A$\beta_{42}$ were also associated with risk, AAO, and/or progression (Table 3). The *GLIS1* locus was associated with lower CSF A$\beta_{42}$ levels (rs185031519[G], $\beta = -0.059$, $P = 2.08 \times 10^{-8}$), increased AD risk (rs114122417[A], OR = 1.105, $P = 0.034$) [48], and faster disease progression (rs185031519[G], $\beta = 0.277$, $P = 0.019$) (Table 3). The intronic *SERPINB1* variant, rs316341[G], was associated with earlier AAO ($\beta = 0.043$, $P = 4.62 \times 10^{-3}$) as well as lower A$\beta_{42}$ ($\beta = -0.025$, $P = 1.72 \times 10^{-8}$) (Table 3). Although the loci associated with ptau$_{181}$ that we reported previously were associated with AD risk and AAO [13], we did not find evidence that the novel loci were associated with risk, AAO, or progression (Table 3). We were unable to test other AD phenotypes such as brain atrophy or neuropathology. However, both the *MAPT* locus on 17q21, which is associated with CSF tau levels in the presence of A$\beta$ deposition [45], and the *GMNC* locus, which was associated with CSF levels of tau ($\beta = 0.040$, $P = 3.07 \times 10^{-11}$) and ptau$_{181}$ ($\beta = 0.035$, $P = 7.62 \times 10^{-10}$), as well as AD risk (OR = 1.044, $P = 9.08 \times 10^{-3}$),

tangle pathology ($P = 0.039$, reported previously) and cognitive decline ($P = 4.86 \times 10^{-5}$, reported previously) [13], have recently been associated with total brain volume in a meta-analysis of 26,577 individuals of European descent [1], suggesting variants associated with ptau$_{181}$ may also be associated with other brain-related or neurodegenerative phenotypes.

### Bioinformatics annotation

None of the genotyped or imputed SNPs in the genome-wide significant loci for Aβ$_{42}$ or ptau$_{181}$ were coding variants ($R^2 > 0.5$, Supplementary Tables 3, 4). In an effort to pinpoint functional genes influencing CSF protein levels, we searched for SNPs in the genome-wide significant loci with *cis* expression quantitative trait locus (eQTL) effects in human tissues. The top SNPs associated with Aβ$_{42}$ on 6p25 have eQTL effects for *SERPINB1* in transformed fibroblasts (rs316341[G]: $\beta = 0.24$, $P = 1.3 \times 10^{-7}$) and whole blood (rs316339[A]: $Z$ score = 28.96, $P = 2.2 \times 10^{-184}$), and rs316339 had the strongest eQTL effect on *SERPINB1* in the hippocampus ($\beta = 0.30$, $P = 3.90 \times 10^{-5}$) (Table 4). To determine if the putative causal variant is the same for *SERPINB1* expression and Aβ$_{42}$ levels, we utilized Summary data-based Mendelian Randomization (SMR) [85] to test the Westra whole blood expression data [79]. One *SERPINB1* variant, rs316339, which is in LD with rs316341 ($D' = 1$, $r^2 = 0.993$; CSF Aβ$_{42}$ $\beta = -0.025$, $P = 1.76 \times 10^{-8}$), passed the SMR analysis ($P = 2.95 \times 10^{-8}$) and HEIDI test ($P = 0.258$). We performed the same test on macrophage expression data obtained from Cardiogenics and rs316341 passed the SMR analysis ($P = 1.23 \times 10^{-7}$) and HEIDI test ($P = 0.240$). This suggests that the locus associated with CSF Aβ$_{42}$ is the same locus that affects expression of *SERPINB1* in blood and macrophages.

The other genetic loci for Aβ$_{42}$ and ptau$_{181}$ were not as enriched for significant eQTL effects as *SERPINB1*, but there were suggestive results for 1p32.3 (near *GLIS1*) and 18q23 (near *CTDP1*). The signal near *GLIS1* associated with Aβ$_{42}$ (1p32.3) had an eQTL effect on *SLC1A7* throughout the brain (rs185031519[G]: $P = 8.8 \times 10^{-5}$); however, overall expression of *SLC1A7* was reported to be relatively low in the human brain, within the 33$^{\text{rd}}$ percentile of all gene expression in the temporal cortex, primarily in endothelial cells [84] (Supplementary Table 13). The locus on 18q23 associated with ptau$_{181}$, between *CTDP1* and *NFATC1*, may have eQTL effects on both genes in the frontal cortex (rs12961169[T]: *CTDP1*, $\beta = -0.319$, $P = 3.85 \times 10^{-5}$ ; *NFATC1*, $\beta = -0.290$, $P = 1.71 \times 10^{-5}$). Both *NFATC1* and *CTDP1* are expressed in the human temporal cortex (*NFATC1* = 58th percentile; *CTDP1* = 37th percentile; Supplementary Table 13).

### Effect of AD risk loci on CSF levels

We wanted to determine whether known loci for AD risk are also associated with CSF levels of Aβ$_{42}$ or ptau$_{181}$. AD risk variants identified in the IGAP study [48] that were most significantly associated with Aβ$_{42}$ were located in the *CLU* ($\beta = 0.014$, $P = 0.001$) and *FERMT2* ($\beta = -0.018$, $P = 0.009$) gene regions, and SNPs in the *CELF1* and *ABCA7* regions had $P < 0.05$ (Supplementary Table 11). For CSF ptau$_{181}$ levels, the most significant association was in the *INPP5D* region ($\beta = 0.014$, $P = 0.009$) and the *CR1, PICALM*, and *FERMT2* regions had $P < 0.05$ (Supplementary Table 11). These results suggest that the risk variant in the *CLU* locus (rs11136000[T]) may increase risk for AD through an Aβ-

associated mechanism and the *INPP5D* locus by a ptau-associated mechanism. Other loci like *APOE* or *FERMT2* may act through both Aβ- and ptau-associated pathways to affect AD risk, and still other risk loci may act through alternate mechanisms such as neuronal survival, apoptosis, or homeostasis.

Although the individual AD risk variants were not strongly associated with $A\beta_{42}$ or $ptau_{181}$, we decided to analyze the potential overlap in the genetic architecture of AD risk and these endophenotype levels by determining whether PRS (with or without the effect of *APOE* genotype) calculated from the genome-wide significant hits for AD risk are also associated with CSF levels. We found not only a strong association between the non-*APOE* PRS and $A\beta_{42}$ ($\beta = -0.033$, $P = 5.01 \times 10^{-7}$), but also tau ($\beta = 0.049$, $P = 1.38 \times 10^{-7}$) and $ptau_{181}$ ($\beta = 0.049$, $P = 1.81 \times 10^{-8}$) (Supplementary Table 11). The strength of the association with the *non-APOE* PRS was greater than any of the individual SNPs composing the PRS. The addition of *APOE* genotype significantly increased the PRS association with CSF levels ($A\beta_{42}$: $\beta = -0.065$, $P = 5.01 \times 10^{-88}$; tau: $\beta = 0.051$, $P = 1.38 \times 10^{-31}$; and $ptau_{181}$: $\beta = 0.044$, $P = 1.81 \times 10^{-31}$) (Supplementary Table 11).

### Estimation of CSF level variance explained by associated genetic loci

To determine the proportion of phenotypic variance ($h^2$) explained by the genetic loci identified for $A\beta_{42}$ and $ptau_{181}$, we analyzed all of the tested genotyped and imputed autosomal common variants (MAF > 0.02). It was recently demonstrated that estimated $h^2$ may be biased if causal variants are enriched in areas with lower or higher LD than average [81], so we used the GCTA tool to calculate segment-based LD scores (segment length = 200 kb) for all SNPs and plotted the number of SNPs with $P < 1 \times 10^{-5}$ for $A\beta_{42}$ and $ptau_{181}$ (Supplementary Fig. 12). Since we observed LD heterogeneity in the associated variants, and the LDMS method can be applied to imputed GWAS data, we used the GCTA LDMS method to test all SNPs in our genetic data [81]. After correcting for age, sex, and two principal components, approximately 35.5% of the variability in $A\beta_{42}$ and 24.9% in $ptau_{181}$ levels were explained by common variants; the respective SNPs associated with CSF $A\beta_{42}$ and $ptau_{181}$ with $P < 1 \times 10^{-5}$ only accounted for 3.5% (2.9% from chromosome 19) of the variability in $A\beta_{42}$ levels and 3.2% (1.4% from chromosome 19) in $ptau_{181}$ levels, corresponding to 10 and 13% of the estimated $h^2$ for CSF $A\beta_{42}$ and $ptau_{181}$, respectively. These results suggest many genetic variants have yet to be discovered.

## Discussion

Genetic studies using disease endophenotypes as quantitative traits provide power to identify loci associated with disease risk with smaller sample sizes, and endophenotypes provide biological context to help identify loci associated with other disease phenotypes such as AAO and disease progression. In our previous study using CSF levels of $A\beta_{42}$ and $ptau_{181}$ as endophenotypes, rs9877502 (near *GMNC1* on 3q28) was reported, for the first time, to be associated with $ptau_{181}$ levels, AD risk, tangle pathology, and cognitive decline [13]. The $ptau_{181}$ association was recently replicated in an independent cohort [63] and we confirmed the association in this much larger dataset. The *GMNC1* locus was also recently reported to be associated with intracranial volume [1], suggesting that tau-associated pathology and

brain volume share some genetic architecture. This larger study also revealed novel loci associated not only with $A\beta_{42}$ but also with AD risk and disease progression (rs185031519[G], (rs185031519[G], $P = 3.43 \times 10^{-2}$ and $P = 1.92 \times 10^{-2}$, respectively), or AAO (rs316341[G], $P = 4.62 \times 10^{-3}$). The associations with AD risk and AAO were tested in independent datasets. The associations of these SNPs with risk, disease progression, and AAO may not pass stringent multiple test correction if we take into account the number of SNPs and phenotypes tested. However, it is important to note that we had a very specific hypothesis, including direction of effect, for each SNP. As expected, the alleles associated with lower CSF levels of $A\beta_{42}$ were also associated with earlier disease symptom onset, increased AD risk, or faster progression. In any case, the associations with risk, disease progression, and AAO were identified in the largest datasets available to date, but additional studies will be needed to confirm the role of these loci in AD. By increasing the sample size more than twofold, we not only verified the results from our previous analyses, but also uncovered additional findings that can be used to inform future AD studies.

*APOE* genotype is the strongest genetic risk factor for sporadic AD, and is consistently the strongest association with CSF levels of $A\beta_{42}$, tau, and $ptau_{181}$ in several GWAS as well [13, 36, 46, 63]. Numerous studies have explored how *APOE* influences amyloid pathology in AD [67]. A few studies have also looked at the role of ApoE in tau pathology [30, 49, 52]. A recent study of brain tissue from 1056 individuals (659 AD cases) found that the *APOE ε4* and *ε2* alleles were not associated with tau tangle pathology in the absence of amyloid deposits [27]. As we previously reported, after accounting for CSF $A\beta_{42}$, there was a strong association for *APOE* with CSF $ptau_{181}$, although it no longer passed genome-wide significance [13]. We verified these results in the current study, and with the larger dataset the *APOE* signal remained genome-wide significant after accounting for $A\beta_{42}$ levels. This provides additional evidence that *APOE* influences $ptau_{181}$-associated mechanisms of AD independently of $A\beta_{42}$-associated mechanisms. We also found, through conditional analyses, that although *APOE* genotype is driving most of the association for *APOE* with CSF $A\beta_{42}$ and $ptau_{181}$, there appears to be an additional signal within the *APOE* gene region that is independent of *APOE ε2, ε3,* and *ε4*.

CSF $A\beta_{42}$ and $ptau_{181}$ are well-established AD endophenotypes with a clear common genetic association for *APOE* and AD risk, but the shared genetic architecture between the disease and AD biomarkers is not as well-understood [7, 13–15]. Shared heritability between two traits can be estimated using different methods to calculate genetic and phenotypic correlations by linear mixed models, LD scoring, or genome partitioning; but most methods currently available usually require sample sizes in the tens of thousands to counteract statistical noise [3, 9, 10, 12, 66]. Another method to detect shared genetic etiology between traits is to calculate a PRS from a well-characterized cohort, usually from large case–control GWAS, and regress the other trait of interest, such as CSF protein levels, on the PRS in an independent cohort [21, 24]. Small studies ($N < 350$) have found that PRS were negatively correlated with CSF $A\beta_{42}$ but not correlated with tau or $ptau_{181}$ [54, 65, 71]. Recent studies of AD cases ($N = 338$) or individuals with mild cognitive impairment ($N = 454$), reported that their PRS without *APOE* were not associated with $A\beta_{42}$, but tau and ptau were associated with the score without the *APOE* effect [53, 71]. In our current study of both AD cases and controls ($N = 3145$), we calculated a PRS composed of genome-wide

significant AD risk loci that were reported in the largest AD case–control GWAS thus far [48]. Since the *APOE* locus is strongly associated with CSF levels and AD risk, it is not unexpected that PRS that include *APOE* effect would also be significantly associated with $A\beta_{42}$ and $ptau_{181}$. Calculating PRS without including the *APOE* effect can provide information about the much smaller genetic effect of other AD risk loci, and although the individual variants were not even suggestively significant the PRS was significantly associated with both proteins. This suggests there is a genetic overlap between AD risk and the CSF biomarkers that is not apparent in single variant analyses. Since we restricted the PRS to genome-wide significant AD risk loci, we may actually be underestimating genetic overlap between AD risk and CSF $A\beta_{42}$ and $ptau_{181}$. Some of the AD risk loci did not appear to be associated with either biomarker, suggesting they affect AD risk through mechanisms independent of $A\beta_{42}$ and $ptau_{181}$. Some AD risk loci such as *CLU* and *PERMT2* for $A\beta_{42}$ and *INPP5D* for $ptau_{181}$ may be associated with these AD endophenotypes but did not reach genome-wide significance. Reasons for this could be that multiple risk loci interact to influence CSF levels, or possibly a lack of power due to small effect size of the individual variants. For example, we estimated that at least 4500 samples would be necessary for the association for *CLU* with $A\beta_{42}$ to pass the genome-wide significance threshold ($P < 5 \times 10^{-8}$), suggesting that additional signals could be identified with a larger sample size.

Genetic studies of endophenotypes not only provide enough power to identify novel associations with smaller sample sizes than case–control studies, but can also help with understanding biological mechanisms of disease. Loci identified in this study alter gene expression or protein binding, which can provide valuable information for understanding the biological basis for AD pathology. We identified here, for the first time, two genome-wide significant signals for CSF $A\beta_{42}$ outside the *APOE* region. Of particular interest is the locus on 6p25 which is associated with lower CSF $A\beta_{42}$ and earlier AAO. This may be mediated through *SERPINB1*, because the same SNPs affect *SERPINB1* expression in blood and macrophages. *SERPINB1* encodes a serine protease inhibitor that is a key regulator of neutrophil programmed cell death [28, 50]. *SERPINB1* is expressed in the human brain, primarily in microglia and macrophages [84]. Recent research of transgenic mouse models for AD (5×FAD and 3×Tg-AD) reported that neutrophils were present in the brain near $A\beta$ deposits, and researchers observed neutrophil migration from blood into the brain toward amyloid plaques [4, 83]. They discovered that $A\beta_{42}$ triggered the high-affinity state of integrin LFA-1, which is necessary for neutrophil infiltration of the CNS [83]. Their results, combined with our findings that genetic variants that increase expression of *SERPINB1* are also associated with lower levels of $A\beta_{42}$, support other studies suggesting that immune response pathways may play a key role in AD pathology [38, 75]. Our results indicate a potential role for *SER-PINB1* in AD and suggest that adaptive immune response mechanisms are associated with $A\beta$-mediated pathology. Key proteins in neuroinflammation, triggering receptor expressed on myeloid cells 2 (TREM2) and YKL-40, are promising AD biomarkers [59, 60], and *TREM2* variants are also strongly associated with AD risk [6, 34, 42]. Clusterin (*CLU*) has been associated with AD risk in numerous studies [37, 48] and a GWAS of CSF CLU levels suggested CLU may be associated with immune response [20]. Our findings add to this growing evidence that

immune response plays a key role in AD and CSF levels of $A\beta_{42}$ may be representative of this role.

The associations of the *GMNC* locus with $ptau_{181}$ levels and brain volume suggest biological mechanisms other than immune response may be associated with tau-mediated pathology in AD [1, 13, 63]. Although not well studied, *GMNC* (also known as *GEMC1*) is a necessary regulator of DNA replication [5] and recently was shown to be a key player in the differentiation of radial glial cells to multiciliated neuroepithelial cells during neurogenesis in the sub-ventricular zone [47]. Combined with our GWAS results, it appears *GMNC* may influence CSF $ptau_{181}$ as part of the neurogenesis process. Further research is needed to determine if *GMNC* is indeed the gene affecting $ptau_{181}$ and what biological mechanism is involved. However, some of the loci associated with $ptau_{181}$ suggest immune response may also play a role in tau-associated pathology. *NFATC1* encodes the nuclear factor of activated T-cells cytoplasmic 1 protein which is important in gene transcription induced by immune response. *CTDP1* encodes the RNA polymerase II subunit A C-terminal domain phosphatase which interacts with the TFIIF transcription factor. Both *NFATC1* and *CTDP1* are expressed in the human temporal cortex, *NFATC1* (58th percentile) more so than *CTDP1* (37th percentile). *NFATC1* is also the more promising candidate than *CTDP1* because *CTDP1* is primarily expressed in fetal astrocytes and nominally in other cell types, while *NFATC1* is predominantly expressed in microglia and macrophages [84] (Supplementary Table 13). We were unable to test for the putative causal variant in these regions for these eQTL effects. However, these data suggest the top loci may influence $ptau_{181}$ levels by affecting expression of these genes.

In summary, by increasing the sample size more than twofold we not only verified the results from our previous analyses, but also uncovered additional findings that can be used to inform future AD studies. We identified novel associations between genetic loci and CSF levels that may provide insight into the biological mechanisms that affect protein levels, influence AD risk, AAO, and disease progression. Our findings suggest CSF $A\beta_{42}$ levels may be representative of the role of immune response on $A\beta$-associated pathology, and that this role may influence AAO. Although immune-related genes may be associated with $ptau_{181}$, our results suggest that CSF $ptau_{181}$ may reflect pathways related to neurogenesis and brain volume. Although we did not identify individual AD risk variants outside the *APOE* region, the PRS results indicate shared genetic architecture between AD risk and these CSF biomarkers. Larger studies using AD endophenotypes will likely provide even more information to help understand the biology underlying AD pathology.

## Supplementary Material

Refer to Web version on PubMed Central for supplementary material.

## Acknowledgments

# References

1. Adams HH, Hibar DP, Chouraki V, Stein JL, Nyquist PA, Renteria ME, Trompet S, Arias-Vasquez A, Seshadri S, Desrivieres S, et al. Novel genetic loci underlying human intracranial volume identified through genome-wide association. Nat Neurosci. 2016; doi: 10.1038/nn.4398

2. Andersson C, Blennow K, Almkvist O, Andreasen N, Engfeldt P, Johansson SE, Lindau M, Eriksdotter-Jonhagen M. Increasing CSF phosphotau levels during cognitive decline and progression to dementia. Neurobiol Aging. 2008; 29:1466–1473. DOI: 10.1016/j.neurobiolaging.2007.03.027 [PubMed: 17512092]

3. Anttila V, Bulik-Sullivan B, Finucane HK, Bras J, Duncan L, Escott-Price V, Falcone G, Gormley P, Malik R, Patsopoulos N, et al. Analysis of shared heritability in common disorders of the brain. bioRxiv. 2016; doi: 10.1101/048991

4. Baik SH, Cha MY, Hyun YM, Cho H, Hamza B, Kim DK, Han SH, Choi H, Kim KH, Moon M, et al. Migration of neutrophils targeting amyloid plaques in Alzheimer's disease mouse model. Neurobiol Aging. 2014; 35:1286–1292. DOI: 10.1016/j.neurobiolaging.2014.01.003 [PubMed: 24485508]

5. Balestrini A, Cosentino C, Errico A, Garner E, Costanzo V. GEMC1 is a TopBP1-interacting protein required for chromosomal DNA replication. Nat Cell Biol. 2010; 12:484–491. DOI: 10.1038/ncb2050 [PubMed: 20383140]

6. Benitez BA, Cooper B, Pastor P, Jin SC, Lorenzo E, Cervantes S, Cruchaga C. TREM2 is associated with the risk of Alzheimer's disease in Spanish population. Neurobiol Aging. 2013; 34(1711):e1715–e1717. DOI: 10.1016/j.neurobiolaging.2012.12.018

7. Blennow K, Hampel H, Weiner M, Zetterberg H. Cerebrospinal fluid and plasma biomarkers in Alzheimer disease. Nat Rev Neurol. 2010; 6:131–144. DOI: 10.1038/nrneurol.2010.4 [PubMed: 20157306]

8. Boyle AP, Hong EL, Hariharan M, Cheng Y, Schaub MA, Kasowski M, Karczewski KJ, Park J, Hitz BC, Weng S, et al. Annotation of functional variation in personal genomes using RegulomeDB. Genome Res. 2012; 22:1790–1797. DOI: 10.1101/gr.137323.112 [PubMed: 22955989]

9. Bulik-Sullivan B, Finucane HK, Anttila V, Gusev A, Day FR, Loh PR, Duncan L, ReproGen C, et al. Psychiatric Genomics C, Genetic Consortium for Anorexia Nervosa of the Wellcome Trust Case Control C. An atlas of genetic correlations across human diseases and traits. Nat Genet. 2015; 47:1236–1241. DOI: 10.1038/ng.3406 [PubMed: 26414676]

10. Bulik-Sullivan BK, Loh PR, Finucane HK, Ripke S, Yang J, Patterson N, Daly MJ, Price AL, Neale BM. Schizophrenia Working Group of the Psychiatric Genomics C. LD Score regression distinguishes confounding from polygenicity in genome-wide association studies. Nat Genet. 2015; 47:291–295. DOI: 10.1038/ng.3211 [PubMed: 25642630]

11. Chang CC, Chow CC, Tellier LC, Vattikuti S, Purcell SM, Lee JJ. Second-generation PLINK: rising to the challenge of larger and richer datasets. Gigascience. 2015; 4:7.doi: 10.1186/s13742-015-0047-8 [PubMed: 25722852]

12. Cross-Disorder Group of the Psychiatric Genomics C. Genetic relationship between five psychiatric disorders estimated from genome-wide SNPs. Nat Genet. 2013; 45:984–994. DOI: 10.1038/ng.2711 [PubMed: 23933821]

13. Cruchaga C, Kauwe JS, Harari O, Jin SC, Cai Y, Karch CM, Benitez BA, Jeng AT, Skorupa T, Carrell D, et al. GWAS of cerebrospinal fluid tau levels identifies risk variants for Alzheimer's disease. Neuron. 2013; 78:256–268. DOI: 10.1016/j.neuron.2013.02.026 [PubMed: 23562540]

14. Cruchaga C, Kauwe JS, Mayo K, Spiegel N, Bertelsen S, Nowotny P, Shah AR, Abraham R, Hollingworth P, Harold D, et al. SNPs associated with cerebrospinal fluid phosphotau levels influence rate of decline in Alzheimer's disease. PLoS Genet. 2010; 6:e1001101.doi: 10.1371/journal.pgen.1001101 [PubMed: 20862329]

15. Cruchaga C, Kauwe JS, Nowotny P, Bales K, Pickering EH, Mayo K, Bertelsen S, Hinrichs A, et al. Alzheimer's Disease Neuroimaging I, Fagan AM. Cerebrospinal fluid APOE levels: an endophenotype for genetic studies for Alzheimer's disease. Hum Mol Genet. 2012; 21:4558–4571. DOI: 10.1093/hmg/dds296 [PubMed: 22821396]

16. de Leon MJ, DeSanti S, Zinkowski R, Mehta PD, Pratico D, Segal S, Clark C, Kerkman D, DeBernardis J, Li J, et al. MRI and CSF studies in the early diagnosis of Alzheimer's disease. J Intern Med. 2004; 256:205–223. DOI: 10.1111/j.1365-2796.2004.01381.x [PubMed: 15324364]

17. De Meyer G, Shapiro F, Vanderstichele H, Vanmechelen E, Engelborghs S, De Deyn PP, Coart E, Hansson O, Minthon L, Zetterberg H, et al. Diagnosis-independent Alzheimer disease biomarker signature in cognitively normal elderly people. Arch Neurol. 2010; 67:949–956. DOI: 10.1001/archneurol.2010.179 [PubMed: 20697045]

18. Delaneau O, Marchini J, Consortium GP. Integrating sequence and array data to create an improved 1000 Genomes Project haplotype reference panel. Nat Commun. 2014; doi: 10.1038/ncomms4934

19. Deming Y, Xia J, Cai Y, Lord J, Del-Aguila JL, Fernandez MV, Carrell D, Black K, Budde J, Ma S, et al. Genetic studies of plasma analytes identify novel potential biomarkers for several complex traits. Scientific Reports. 2016; 6:18092.doi: 10.1038/srep18092

20. Deming Y, Xia J, Cai Y, Lord J, Holmans P, Bertelsen S, Holtzman D, Morris JC, Bales K, Pickering EH, et al. A potential endophenotype for Alzheimer's disease: cerebrospinal fluid clusterin. Neurobiol Aging. 2016; 37(208):e201–e209. DOI: 10.1016/j.neurobiolaging.2015.09.009

21. Dudbridge F. Polygenic epidemiology. Genet Epidemiol. 2016; 40:268–272. DOI: 10.1002/gepi.21966 [PubMed: 27061411]

22. Escott-Price V, Shoai M, Pither R, Williams J, Hardy J. Polygenic score prediction captures nearly all common genetic risk for Alzheimer's disease. Neurobiol Aging. 2017; 49 214-e217-214-e211. doi: 10.1016/j.neurobiolaging.2016.07.018

23. Escott-Price V, Sims R, Bannister C, Harold D, Vronskaya M, Majounie E, Badarinarayan N, Gerad Perades, Morgan K, et al. Gerad/Perades, consortia I, Consortia I. Common polygenic variation enhances risk prediction for Alzheimer's disease. Brain. 2015; 138:3673–3684. DOI: 10.1093/brain/awv268 [PubMed: 26490334]

24. Euesden J, Lewis CM, O'Reilly PF. PRSice: polygenic Risk Score software. Bioinformatics. 2015; 31:1466–1468. DOI: 10.1093/bioinformatics/btu848 [PubMed: 25550326]

25. Fagan AM, Head D, Shah AR, Marcus D, Mintun M, Morris JC, Holtzman DM. Decreased cerebrospinal fluid Aβ(42) correlates with brain atrophy in cognitively normal elderly. Ann Neurol. 2009; 65:176–183. DOI: 10.1002/ana.21559 [PubMed: 19260027]

26. Fagan AM, Roe CM, Xiong C, Mintun MA, Morris JC, Holtzman DM. Cerebrospinal fluid tau/β-amyloid(42) ratio as a prediction of cognitive decline in nondemented older adults. Arch Neurol. 2007; 64:343–349. DOI: 10.1001/archneur.64.3.noc60123 [PubMed: 17210801]

27. Farfel JM, Yu L, De Jager PL, Schneider JA, Bennett DA. Association of APOE with tau-tangle pathology with and without β-amyloid. Neurobiol Aging. 2016; 37:19–25. DOI: 10.1016/j.neurobiolaging.2015.09.011 [PubMed: 26481403]

28. Farley K, Stolley JM, Zhao P, Cooley J, Remold-O'Donnell E. A serpinB1 regulatory mechanism is essential for restricting neutrophil extracellular trap generation. J Immunol. 2012; 189:4574–4581. DOI: 10.4049/jimmunol.1201167 [PubMed: 23002442]

29. Farrer LA, Cupples L, Haines JL, et al. Effects of age, sex, and ethnicity on the association between apolipoprotein e genotype and alzheimer disease: a meta-analysis. JAMA. 1997; 278:1349–1356. DOI: 10.1001/jama.1997.03550160069041 [PubMed: 9343467]

30. Fleming LM, Weisgraber KH, Strittmatter WJ, Troncoso JC, Johnson GV. Differential binding of apolipoprotein E isoforms to tau and other cytoskeletal proteins. Exp Neurol. 1996; 138:252–260. DOI: 10.1006/exnr.1996.0064 [PubMed: 8620924]

31. Gatz M, Reynolds CA, Fratiglioni L, Johansson B, Mortimer JA, Berg S, Fiske A, Pedersen NL. Role of genes and environments for explaining Alzheimer disease. Arch Gen Psychiat. 2006; 63:168–174. DOI: 10.1001/archpsyc.63.2.168 [PubMed: 16461860]

32. Grundberg E, Adoue V, Kwan T, Ge B, Duan QL, Lam KCL, Koka V, Kindmark A, Weiss ST, Tantisira K, et al. Global analysis of the impact of environmental perturbation on cis-regulation of gene expression. PLoS Genet. 2011; doi: 10.1371/journal.pgen.1001279

33. GTEx Consortium. Human genomics. The Genotype-Tissue Expression (GTEx) pilot analysis: multitissue gene regulation in humans. Science. 2015; 348:648–660. DOI: 10.1126/science.1262110 [PubMed: 25954001]

34. Guerreiro R, Wojtas A, Bras J, Carrasquillo M, Rogaeva E, Majounie E, Cruchaga C, Sassi C, Kauwe JSK, Lupton MK, et al. TREM2 variants in Alzheimer's disease. New Engl J Med. 2013; 368:117–127. DOI: 10.1056/NEJMoa1211851 [PubMed: 23150934]

35. Guo H, Fortune MD, Burren OS, Schofeld E, Todd JA, Wallace C. Integration of disease association and eQTL data using a Bayesian colocalisation approach highlights six candidate causal genes in immune-mediated diseases. Hum Mol Genet. 2015; 24:3305–3313. DOI: 10.1093/hmg/ddv077 [PubMed: 25743184]

36. Han MR, Schellenberg GD, Wang LS. Alzheimer's Disease Neuroimaging I. Genome-wide association reveals genetic effects on human Aβ42 and tau protein levels in cerebrospinal fluids: a case control study. BMC Neurol. 2010; 10:90.doi: 10.1186/1471-2377-10-90 [PubMed: 20932310]

37. Harold D, Abraham R, Hollingworth P, Sims R, Gerrish A, Hamshere ML, Pahwa JS, Moskvina V, Dowzell K, Williams A, et al. Genome-wide association study identifies variants at CLU and PICALM associated with Alzheimer's disease (vol 41, pg 1088, 2009). Nat Genet. 2009; 41:1156.doi: 10.1038/ng1009-1156d

38. Heppner FL, Ransohoff RM, Becher B. Immune attack: the role of inflammation in Alzheimer disease. Nat Rev Neurosci. 2015; 16:358–372. DOI: 10.1038/nrn3880 [PubMed: 25991443]

39. Hollingworth P, Harold D, Sims R, Gerrish A, Lambert JC, Carrasquillo MM, Abraham R, Hamshere ML, Pahwa JS, Moskvina V, et al. Common variants at ABCA7, MS4A6A/MS4A4E, EPHA1, CD33 and CD2AP are associated with Alzheimer's disease. Nat Genet. 2011; 43:429–435. DOI: 10.1038/ng.803 [PubMed: 21460840]

40. Howie B, Fuchsberger C, Stephens M, Marchini J, Abecasis GR. Fast and accurate genotype imputation in genome-wide association studies through pre-phasing. Nat Genet. 2012; 44:955.doi: 10.1038/ng.2354 [PubMed: 22820512]

41. Hulette CM, Welsh-Bohmer KA, Murray MG, Saunders AM, Mash DC, McIntyre LM. Neuropathological and neuropsychological changes in "normal" aging: evidence for preclinical

Alzheimer disease in cognitively normal individuals. J Neuropathol Exp Neurol. 1998; 57:1168–1174. [PubMed: 9862640]

42. Jonsson T, Stefansson H, Steinberg S, Jonsdottir I, Jonsson PV, Snaedal J, Bjornsson S, Huttenlocher J, Levey AI, Lah JJ, et al. Variant of TREM2 associated with the risk of Alzheimer's disease. New Engl J Med. 2013; 368:107–116. DOI: 10.1056/NEJMoa1211103 [PubMed: 23150908]

43. Kanai M, Matsubara E, Isoe K, Urakami K, Nakashima K, Arai H, Sasaki H, Abe K, Iwatsubo T, Kosaka T, et al. Longitudinal study of cerebrospinal fluid levels of tau, A beta1-40, and A beta1-42(43) in Alzheimer's disease: a study in Japan. Ann Neurol. 1998; 44:17–26. DOI: 10.1002/ana.410440108 [PubMed: 9667589]

44. Kauwe JS, Cruchaga C, Bertelsen S, Mayo K, Latu W, Nowotny P, Hinrichs AL, Fagan AM, Holtzman DM, et al. Alzheimer's Disease Neuroimaging I. Validating predicted biological effects of Alzheimer's disease associated SNPs using CSF biomarker levels. J Alzheimers Dis. 2010; 21:833–842. DOI: 10.3233/JAD-2010-091711 [PubMed: 20634593]

45. Kauwe JS, Cruchaga C, Mayo K, Fenoglio C, Bertelsen S, Nowotny P, Galimberti D, Scarpini E, Morris JC, Fagan AM, et al. Variation in MAPT is associated with cerebrospinal fluid tau levels in the presence of amyloid-beta deposition. Proc Natl Acad Sci USA. 2008; 105:8050–8054. DOI: 10.1073/pnas.0801227105 [PubMed: 18541914]

46. Kim S, Swaminathan S, Shen L, Risacher SL, Nho K, Foroud T, Shaw LM, Trojanowski JQ, Potkin SG, Huentelman MJ, et al. Genome-wide association study of CSF biomarkers Aβ1-42, t-tau, and p-tau181p in the ADNI cohort. Neurology. 2011; 76:69–79. DOI: 10.1212/WNL.0b013e318204a397 [PubMed: 21123754]

47. Kyrousi C, Arbi M, Pilz GA, Pefani DE, Lalioti ME, Ninkovic J, Gotz M, Lygerou Z, Taraviras S. Mcidas and GemC1 are key regulators for the generation of multiciliated ependymal cells in the adult neurogenic niche. Development. 2015; 142:3661–3674. DOI: 10.1242/dev.126342 [PubMed: 26395491]

48. Lambert JC, Ibrahim-Verbaas CA, Harold D, Naj AC, Sims R, Bellenguez C, DeStafano AL, Bis JC, Beecham GW, Grenier-Boley B, et al. Meta-analysis of 74,046 individuals identifies 11 new susceptibility loci for Alzheimer's disease. Nat Genet. 2013; 45:1452–1458. DOI: 10.1038/ng.2802 [PubMed: 24162737]

49. Leoni V, Solomon A, Kivipelto M. Links between ApoE, brain cholesterol metabolism, tau and amyloid β-peptide in patients with cognitive impairment. Biochem Soc Trans. 2010; 38:1021–1025. DOI: 10.1042/BST0381021 [PubMed: 20658997]

50. Lepretre C, Tchakarska G, Blibech H, Lebon C, Torriglia A. Apoptosis-inducing factor (AIF) and leukocyte elastase inhibitor/L-DNase II (LEI/LDNaseII), can interact to conduct caspase-independent cell death. Apoptosis. 2013; 18:1048–1059. DOI: 10.1007/s10495-013-0862-2 [PubMed: 23673989]

51. Li QS, Parrado AR, Samtani MN, Narayan VA. Alzheimer's Disease Neuroimaging I. Variations in the FRA10AC1 Fragile Site and 15q21 Are Associated with Cerebrospinal Fluid Aβ1-42 Level. PLoS ONE. 2015; 10:e0134000.doi: 10.1371/journal.pone.0134000 [PubMed: 26252872]

52. Liraz O, Boehm-Cagan A, Michaelson DM. ApoE4 induces Aβ42, tau, and neuronal pathology in the hippocampus of young targeted replacement apoE4 mice. Mol Neurodegener. 2013; 8:16.doi: 10.1186/1750-1326-8-16 [PubMed: 23684315]

53. Louwersheimer E, Wolfsgruber S, Espinosa A, Lacour A, Heilmann-Heimbach S, Alegret M, Hernandez I, Rosende-Roca M, Tarraga L, Boada M, et al. Alzheimer's disease risk variants modulate endophenotypes in mild cognitive impairment. Alzheimers Dement. 2016; 12:872–881. DOI: 10.1016/j.jalz.2016.01.006 [PubMed: 26921674]

54. Martiskainen H, Helisalmi S, Viswanathan J, Kurki M, Hall A, Herukka SK, Sarajarvi T, Natunen T, Kurkinen KM, Huovinen J, et al. Effects of Alzheimer's disease-associated risk loci on cerebrospinal fluid biomarkers and disease progression: a polygenic risk score approach. J Alzheimers Dis. 2015; 43:565–573. DOI: 10.3233/JAD-140777 [PubMed: 25096612]

55. Morris JC, Price JL. Pathologic correlates of nondemented aging, mild cognitive impairment, and early-stage Alzheimer's disease. J Mol Neurosci. 2001; 17:101–118. [PubMed: 11816784]

56. Naj AC, Jun G, Beecham GW, Wang LS, Vardarajan BN, Buros J, Gallins PJ, Buxbaum JD, Jarvik GP, Crane PK, et al. Common variants at MS4A4/MS4A6E, CD2AP, CD33 and EPHA1 are

associated with late-onset Alzheimer's disease. Nat Genet. 2011; 43:436–441. DOI: 10.1038/ng. 801 [PubMed: 21460841]

57. O'Bryant SE, Lacritz LH, Hall J, Waring SC, Chan W, Khodr ZG, Massman PJ, Hobson V, Cullum CM. Validation of the new interpretive guidelines for the clinical dementia rating scale sum of boxes score in the national Alzheimer's coordinating center database. Arch Neurol. 2010; 67:746–749. DOI: 10.1001/archneurol.2010.115 [PubMed: 20558394]

58. O'Bryant SE, Waring SC, Cullum CM, Hall J, Lacritz L, Massman PJ, Lupo PJ, Reisch JS, Doody R. Texas Alzheimer's Research C. Staging dementia using Clinical Dementia Rating Scale Sum of Boxes scores: a Texas Alzheimer's research consortium study. Arch Neurol. 2008; 65:1091–1095. DOI: 10.1001/archneur.65.8.1091 [PubMed: 18695059]

59. Olsson B, Lautner R, Andreasson U, Ohrfelt A, Portelius E, Bjerke M, Holtta M, Rosen C, Olsson C, Strobel G, et al. CSF and blood biomarkers for the diagnosis of Alzheimer's disease: a systematic review and meta-analysis. Lancet Neurol. 2016; 15:673–684. DOI: 10.1016/S1474-4422(16)00070-3 [PubMed: 27068280]

60. Piccio L, Deming Y, Del-Aguila JL, Ghezzi L, Holtzman DM, Fagan AM, Fenoglio C, Galimberti D, Borroni B, Cruchaga C. Cerebrospinal fluid soluble TREM2 is higher in Alzheimer disease and associated with mutation status. Acta Neuropathol. 2016; 131:925–933. DOI: 10.1007/s00401-016-1533-5 [PubMed: 26754641]

61. Price AL, Patterson NJ, Plenge RM, Weinblatt ME, Shadick NA, Reich D. Principal components analysis corrects for stratification in genome-wide association studies. Nat Genet. 2006; 38:904–909. DOI: 10.1038/ng1847 [PubMed: 16862161]

62. Pruim RJ, Welch RP, Sanna S, Teslovich TM, Chines PS, Gliedt TP, Boehnke M, Abecasis GR, Willer CJ. LocusZoom: regional visualization of genome-wide association scan results. Bioinformatics. 2010; 26:2336–2337. DOI: 10.1093/bioinformatics/btq419 [PubMed: 20634204]

63. Ramirez A, van der Flier WM, Herold C, Ramonet D, Heilmann S, Lewczuk P, Popp J, Lacour A, Drichel D, Louwersheimer E, et al. SUCLG2 identified as both a determinator of CSF Aβ1-42 levels and an attenuator of cognitive decline in Alzheimer's disease. Hum Mol Genet. 2014; 23:6644–6658. DOI: 10.1093/hmg/ddu372 [PubMed: 25027320]

64. Ridge PG, Hoyt KB, Boehme K, Mukherjee S, Crane PK, Haines JL, Mayeux R, Farrer LA, Pericak-Vance MA, Schellen-berg GD, et al. Assessment of the genetic variance of lateonset Alzheimer's disease. Neurobiol Aging. 2016; 41(200):e213–e220. DOI: 10.1016/j.neurobiolaging. 2016.02.024

65. Sabuncu MR, Buckner RL, Smoller JW, Lee PH, Fischl B, Sperling RA. Alzheimer's Disease Neuroimaging I. The association between a polygenic Alzheimer score and cortical thickness in clinically normal subjects. Cereb Cortex. 2012; 22:2653–2661. DOI: 10.1093/cercor/bhr348 [PubMed: 22169231]

66. Sampson JN, Wheeler WA, Yeager M, Panagiotou O, Wang Z, Berndt SI, Lan Q, Abnet CC, Amundadottir LT, Figueroa JD, et al. Analysis of heritability and shared heritability based on genome-wide association studies for thirteen cancer types. J Natl Cancer Inst. 2015; 107:djv279.doi: 10.1093/jnci/djv279 [PubMed: 26464424]

67. Selkoe DJ, Hardy J. The amyloid hypothesis of Alzheimer's disease at 25 years. EMBO Mol Med. 2016; 8:595–608. DOI: 10.15252/emmm.201606210 [PubMed: 27025652]

68. Shabalin AA. Matrix eQTL: ultra fast eQTL analysis via large matrix operations. Bioinformatics. 2012; 28:1353–1358. DOI: 10.1093/bioinformatics/bts163 [PubMed: 22492648]

69. Shaw LM, Vanderstichele H, Knapik-Czajka M, Clark CM, Aisen PS, Petersen RC, Blennow K, Soares H, Simon A, Lewczuk P, et al. Cerebrospinal fluid biomarker signature in Alzheimer's disease neuroimaging initiative subjects. Ann Neurol. 2009; 65:403–413. DOI: 10.1002/ana.21610 [PubMed: 19296504]

70. Skol AD, Scott LJ, Abecasis GR, Boehnke M. Joint analysis is more efficient than replication-based analysis for two-stage genome-wide association studies. Nat Genet. 2006; 38:209–213. DOI: 10.1038/ng1706 [PubMed: 16415888]

71. Sleegers K, Bettens K, De Roeck A, Van Cauwenberghe C, Cuyvers E, Verheijen J, Struyfs H, Van Dongen J, Vermeulen S, Engelborghs S, et al. A 22-single nucleotide polymorphism Alzheimer's disease risk score correlates with family history, onset age, and cerebrospinal fluid Aβ42. Alzheimers Dement. 2015; 11:1452–1460. DOI: 10.1016/j.jalz.2015.02.013 [PubMed: 26086184]

72. Sunderland T, Linker G, Mirza N, Putnam KT, Friedman DL, Kimmel LH, Bergeson J, Manetti GJ, Zimmermann M, Tang B, et al. Decreased β-amyloid1-42 and increased tau levels in cerebrospinal fluid of patients with Alzheimer disease. JAMA. 2003; 289:2094–2103. DOI: 10.1001/jama. 289.16.2094 [PubMed: 12709467]

73. Trabzuni D, Ryten M, Walker R, Smith C, Imran S, Ramasamy A, Weale ME, Hardy J. Quality control parameters on a large dataset of regionally dissected human control brains for whole genome expression studies. J Neurochem. 2011; 119:275–282. DOI: 10.1111/j. 1471-4159.2011.07432.x [PubMed: 21848658]

74. Turner SD. qqman: an R package for visualizing GWAS results using QQ and manhattan plots. bioRxiv. 2014; doi: 10.1101/005165

75. Van Eldik LJ, Carrillo MC, Cole PE, Feuerbach D, Green-berg BD, Hendrix JA, Kennedy M, Kozauer N, Margolin RA, Molinuevo JL, et al. The roles of inflammation and immune mechanisms in Alzheimer's disease. Alzheimer's Dement Transl Res Clin Interv. 2016; 2:99–109. DOI: 10.1016/j.trci.2016.05.001

76. Visscher PM, Hemani G, Vinkhuyzen AA, Chen GB, Lee SH, Wray NR, Goddard ME, Yang J. Statistical power to detect genetic (co)variance of complex traits using SNP data in unrelated samples. PLoS Genet. 2014; 10:e1004269.doi: 10.1371/jour-nal.pgen.1004269 [PubMed: 24721987]

77. Wang K, Li M, Hakonarson H. ANNOVAR: functional annotation of genetic variants from high-throughput sequencing data. Nucleic Acids Res. 2010; 38:e164.doi: 10.1093/nar/gkq603 [PubMed: 20601685]

78. Ward LD, Kellis M. HaploReg: a resource for exploring chromatin states, conservation, and regulatory motif alterations within sets of genetically linked variants. Nucleic Acids Res. 2012; 40:D930–D934. DOI: 10.1093/nar/gkr917 [PubMed: 22064851]

79. Westra HJ, Peters MJ, Esko T, Yaghootkar H, Schurmann C, Kettunen J, Christiansen MW, Fairfax BP, Schramm K, Powell JE, et al. Systematic identification of trans eQTLs as putative drivers of known disease associations. Nat Genet. 2013; 45:1238–U1195. DOI: 10.1038/ng.2756 [PubMed: 24013639]

80. Willer CJ, Li Y, Abecasis GR. METAL: fast and efficient meta-analysis of genome-wide association scans. Bioinformatics. 2010; 26:2190–2191. DOI: 10.1093/bioinformatics/btq340 [PubMed: 20616382]

81. Yang J, Bakshi A, Zhu Z, Hemani G, Vinkhuyzen AAE, Lee SH, Robinson MR, Perry JRB, Nolte IM, van Vliet-Ostaptchouk JV, et al. Genetic variance estimation with imputed variants finds negligible missing heritability for human height and body mass index. Nat Genet. 2015; 47:1114.doi: 10.1038/ng.3390 [PubMed: 26323059]

82. Yang JA, Lee SH, Goddard ME, Visscher PM. GCTA: a tool for genome-wide complex trait analysis. Am J Hum Genet. 2011; 88:76–82. DOI: 10.1016/j.ajhg.2010.11.011 [PubMed: 21167468]

83. Zenaro E, Pietronigro E, Della Bianca V, Piacentino G, Marongiu L, Budui S, Turano E, Rossi B, Angiari S, Dusi S, et al. Neutrophils promote Alzheimer's disease-like pathology and cognitive decline via LFA-1 integrin. Nat Med. 2015; 21:880–886. DOI: 10.1038/nm.3913 [PubMed: 26214837]

84. Zhang Y, Chen K, Sloan SA, Bennett ML, Scholze AR, O'Keeffe S, Phatnani HP, Guarnieri P, Caneda C, Ruderisch N, et al. An RNA-sequencing transcriptome and splicing database of glia, neurons, and vascular cells of the cerebral cortex. J Neurosci. 2014; 34:11929–11947. DOI: 10.1523/JNEUROSCI.1860-14.2014 [PubMed: 25186741]

85. Zhu Z, Zhang F, Hu H, Bakshi A, Robinson MR, Powell JE, Montgomery GW, Goddard ME, Wray NR, Visscher PM, et al. Integration of summary data from GWAS and eQTL studies predicts complex trait gene targets. Nat Genet. 2016; 48:481–487. DOI: 10.1038/ng.3538 [PubMed: 27019110]
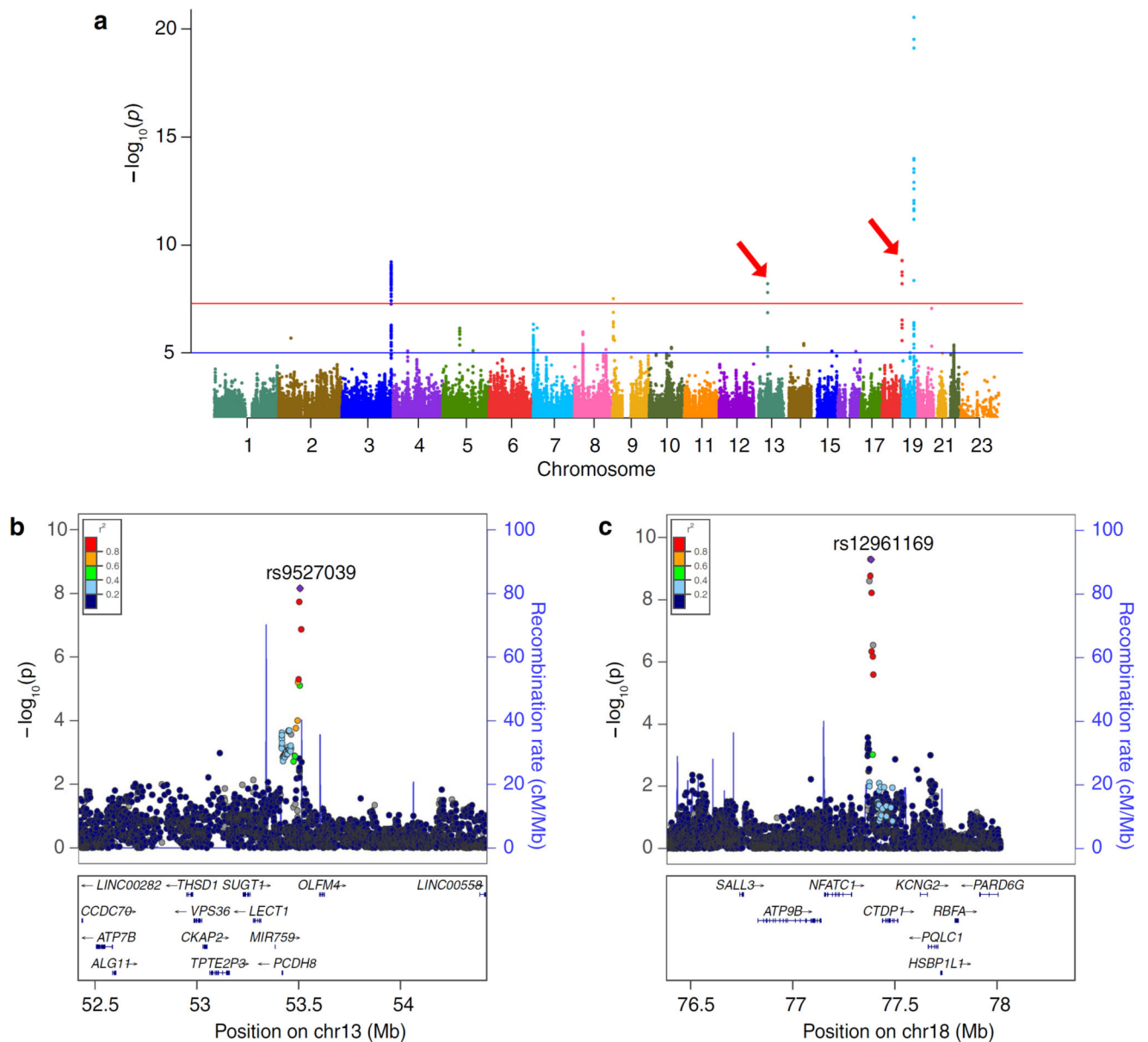
**Fig. 1.**

Association plots from single variant analyses of CSF ptau$_{181}$ levels. **a** Manhattan plot shows negative $\log_{10}$-transformed $P$ values from the joint analysis of ptau$_{181}$. The *horizontal lines* represent the genome-wide significance threshold, $P = 5 \times 10^{-8}$(*red*) and suggestive threshold, $P = 1 \times 10^{-5}$(*blue*). *Red arrows* point to novel loci. The *y*-axis is truncated, the lowest $P$ value on chromosome 19 was $5.30 \times 10^{-33}$.**b, c** Regional association plots of novel loci are shown for SNPs associated with ptau$_{181}$ near *PCDH8* (**a**) and between *NFATC1* and *CTDP1* (**b**). The SNPs labeled on each regional plot had the lowest $P$ value at each locus and are represented by a purple diamond. *Each dot* represents a SNP and *dot colors* indicate LD with the labeled SNP. *Blue vertical lines* show recombination rate marked on the right-hand *y*-axis of each regional plot. *Plots* for previously reported loci are in Supplementary Fig. 7
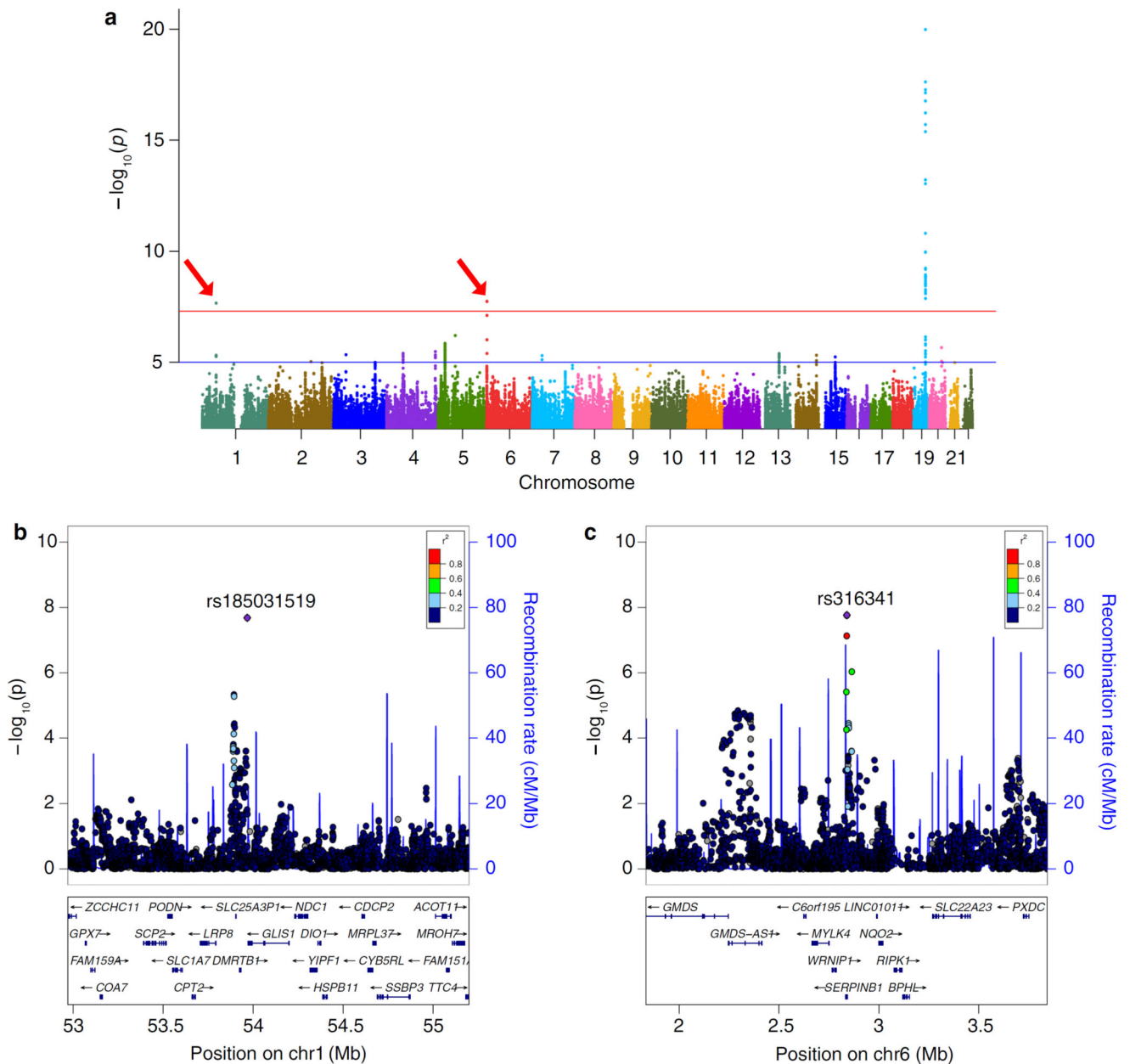
**Fig. 2.**

Association plots from single variant analyses of CSF Aβ$_{42}$. **a** Manhattan plot shows negative log$_{10}$-transformed $P$ values from the joint analysis of Aβ$_{42}$. The *horizontal lines* represent the genome-wide significance threshold, $P = 5 \times 10^{-8}$(*red*) and suggestive threshold, $P = 1 \times 10^{-5}$(*blue*). *Red arrows* point to novel loci. The *y*-axis is truncated, the lowest $P$ value on chromosome 19 was $4.78 \times 10^{-94}$. **b, c** Regional association plots of novel loci are shown for SNPs associated with Aβ$_{42}$ near *GLIS1* (**b**) and within *SERPINB1* (**c**). The SNPs labeled on each regional plot had the lowest $P$ value at each locus and are represented by a purple diamond. *Each dot* represents a SNP and *dot colors* indicate LD with

the labeled SNP. *Blue vertical lines* show recombination rate marked on the right-hand *y*-axis of each regional plot. *Plots* for previously reported loci are in Supplementary Fig. 7

**Table 1**

Cohort demographics

| | Knight ADRC | ADNI1 | ADNI2 | BIOCARD | HB | MAYO | SWEDEN | UPENN | UW |
|---|---|---|---|---|---|---|---|---|---|
| $n = 3146$ | 805 | 390 | 397 | 184 | 105 | 433 | 293 | 164 | 375 |
| Previous study [13] | (501) | (390) | (−) | (−) | (−) | (−) | (−) | (51) | (323) |
| Age (years) | 70.39 ± 9.12 | 77.89 ± 6.89 | 73.28 ± 7.47 | 62.10 ± 9.46 | 67.52 ± 9.24 | 78.73 ± 6.35 | 75.15 ± 7.63 | 71.60 ± 8.98 | 62.35 ± 16 |
| Age range | 37–91 | 58–93 | 55–92 | 23–86 | 45–84 | 50–95 | 50–88 | 50–94 | 21–88 |
| % Male | 46.09 | 60 | 54.91 | 41.53 | 54.29 | 60.51 | 37.54 | 41.46 | 50.67 |
| % APOE e4+ | 40.75 | 50 | 38.29 | 34.43 | 54.29 | 27.5 | 76.11 | 55.56 | 43.28 |
| % CDR > 0 | 29.34 | 71.28 | 71.03 | 5.43 | – | 22.17 | 100 | 62.8 | 33.33 |
| $A\beta_{42}$ levels | 650.40 ± 305.59 | 169.83 ± 56.00 | 179.98 ± 51.31 | 386.90 ± 89.93 | 77.59 ± 23.30 | 331.00 ± 122.21 | 262.43 ± 72.77 | 163.55 ± 53.54 | 141.90 ± 41.42 |
| ptau$_{181}$ levels | 64.94 ± 34.26 | 34.13 ± 18.52 | 38.63 ± 21.21 | 38.94 ± 12.30 | – | 23.16 ± 10.55 | 105.76 ± 41.82 | 36.96 ± 26.80 | 56.56 ± 29.32 |
| Tau levels | 372.40 ± 235.41 | 97.26 ± 52.03 | 79.69 ± 47.79 | 66.56 ± 26.60 | 84.27 ± 36.79 | 104.29 ± 58.06 | 782.20 ± 301.68 | 93.66 ± 54.29 | 61.64 ± 42.77 |

$A\beta_{42}$, ptau$_{181}$, and tau levels are reported as mean ± standard deviation in pg/mL

*Knight ADRC* Charles F and Joanne Knight Alzheimer's Disease Research Center, *ADNI* Alzheimer's Disease Neuroimaging Initiative, *BIO-CARD* Predictors of Cognitive Decline Among Normal Individuals, *HB* Saarland University in Homburg/Saar, Germany, *MAYO* Mayo Clinic. *SWEDEN* Sahlgren's University Hospital, Sweden, *UPENN* Perelman School of Medicine at the University of Pennsylvania, *UW* University of Washington, *CDR* clinical dementia rating

**Table 2**

Results for genome-wide significant loci associated with CSF levels of $A\beta_{42}$, $ptau_{181}$, and tau

| HGVS | SNP[effect allele] | Gene | Function | MAF | $CSFA\beta_{42}$ Beta (SE) | P | CSF $ptau_{181}$ Beta (SE) | P | CSF tau Beta (SE) | P |
|---|---|---|---|---|---|---|---|---|---|---|
| Novel loci | | | | | | | | | | |
| chr1.hg19:g.53968219C>G | rs185031519[G] | GLIS1 | Intergenic | 0.042 | **−0.059 (0.010)** | $2.08 \times 10^{-8}$ | 0.008 (0.015) | $5.94 \times 10^{-1}$ | 0.011(0.015) | $4.72 \times 10^{-1}$ |
| chr6.hg19:g.2838248G>A | rs316341[G] | SERPINB1 | Intronic | 0.302 | **−0.025 (0.004)** | $1.76 \times 10^{-8}$ | 0.007 (0.006) | $2.20 \times 10^{-1}$ | 0.016 (0.006) | $9.19 \times 10^{-3}$ |
| chr13.hg19:g.53504675T>C | rs9527039[C] | PCDH8 | Intergenic | 0.069 | 0.016 (0.008) | $4.24 \times 10^{-2}$ | **−0.061 (0.010)** | $5.95 \times 10^{-9}$ | −0.050(0.011) | $1.10 \times 10^{-5}$ |
| chr18.hg19:g.77381649C>T | rs12961169[T] | CTDP1 | Intergenic | 0.155 | −0.016 (0.006) | $1.13 \times 10^{-2}$ | **0.050 (0.008)** | $5.12 \times 10^{-10}$ | 0.038 (0.009) | $1.37 \times 10^{-5}$ |
| Previously reported loci | | | | | | | | | | |
| chr3.hg19:g.190663557T>C | rs35055419[C] | GMNC | Intergenic | 0.357 | −0.007 (0.004) | $9.71 \times 10^{-2}$ | **0.035 (0.006)** | $7.62 \times 10^{-10}$ | **0.040 (0.006)** | $3.07 \times 10^{-11}$ |
| chr9.hg19:g.3929424C>T | rs514716[C] | GLIS3 | Intronic | 0.125 | 0.007 (0.006) | $2.94 \times 10^{-1}$ | **−0.049 (0.009)** | $2.94 \times 10^{-8}$ | −0.044 (0.009) | $1.36 \times 10^{-6}$ |
| chr19.hg19:g.45410002G>A | rs769449[A] | APOE | Intronic | 0.191 | **−0.101 (0.005)** | $4.78 \times 10^{-94}$ | **0.079 (0.006)** | $5.30 \times 10^{-33}$ | **0.078 (0.007)** | $4.05 \times 10^{-29}$ |

*HGVS* chromosome and base pair position based on Build 37 of reference genome followed by reference allele then alternate allele, *Gene* nearest gene, *MAF* minor allele frequency in our data-set

$\beta$ and *P* values in this table are from the current study. Annotated results from these analyses with $P < 1 \times 10^{-5}$ are shown in Supplementary Tables 2–4 ($P < 5 \times 10^{-8}$ are in bold text)

## Table 3

Genome-wide significant loci from analyses of CSF Aβ$_{42}$ and ptau, associations with AD risk, progression of cognitive decline, and age at disease onset from independent cohorts

| SNP [effect allele] | Gene | MAF | CSF levels $n = 3146$ | | AD risk [48] $n = 74,026$ | | Progression $n = 1530$ | | AAO $n = 39,855$ | |
|---|---|---|---|---|---|---|---|---|---|---|
| | | | β | P | OR | P | β | P | β | P |
| **CSF Aβ$_{42}$ associated loci** | | | | | | | | | | |
| rs185031519[G][a] | *GLIS1* | 0.042 | −0.059 | **2.08 × 10⁻⁸** | 1.105 | **3.43 × 10⁻²[b]** | **0.277** | **1.92 × 10⁻²** | 0.032 | 6.15 × 10⁻¹ |
| rs316341[G][a] | *SERPINB1* | 0.301 | −0.025 | **1.76 × 10⁻⁸** | 1.025 | 1.52 × 10⁻¹[c] | 0.048 | 2.77 × 10⁻¹ | **0.043** | **4.62 × 10⁻³** |
| rs769449[A] | *APOE* | 0.184 | −0.101 | **4.78 × 10⁻⁹⁴** | 3.522 | **9.86 × 10⁻⁵²³** | 0.078 | 8.42 × 10⁻² | **0.720** | **6.81 × 10⁻¹⁰⁶** |
| **CSF ptau$_{181}$ associated loci** | | | | | | | | | | |
| rs35055419[C] | *GMNC* | 0.357 | **0.035** | **7.62 × 10⁻¹⁰** | 1.044 | **9.08 × 10⁻³** | 0.027 | 5.25 × 10⁻¹ | **0.037** | **3.14 × 10⁻³[d]** |
| rs514716[C] | *GLIS3* | 0.125 | −0.049 | **2.94 × 10⁻⁸** | 0.954 | 5.05 × 10⁻² | −0.029 | 6.66 × 10⁻¹ | −0.045 | **1.45 × 10⁻²** |
| rs9527039[C][a] | *PCDH8* | 0.069 | −0.061 | **5.95 × 10⁻⁹** | 0.993 | 8.22 × 10⁻¹ | −0.069 | 4.25 × 10⁻¹ | −0.020 | 4.03 × 10⁻¹ |
| rs12961169[T][a] | *CTDP1* | 0.155 | **0.050** | **5.12 × 10⁻¹⁰** | 1.033 | 1.93 × 10⁻¹ | 0.119 | 9.34 × 10⁻² | 0.042 | 2.49 × 10⁻¹ |
| rs769449[A] | *APOE* | 0.184 | **0.079** | **5.30 × 10⁻³³** | 3.522 | **9.86 × 10⁻⁵²³** | 0.078 | 8.42 × 10⁻² | **0.720** | **6.81 × 10⁻¹⁰⁶** |

*SNP* based on Build 37 of reference genome followed by effect allele, *Gene* nearest gene, *MAF* minor allele frequency in our dataset, *Progression* association with cognitive decline measured by sum of boxes, *AAO* age at onset (personal communication: Huang & Goate)

*P* values below significance threshold are in bold text

[a] Novel associated loci for CSF Aβ42 or ptau[81]

[b] AD risk reported for rs114122417 which is in LD with rs185031519 ($r^2 = 0.909$, $D' = 1$)

[c] AD risk reported for rs316339 which is in LD with rs316341 ($r^2 = 0.993$, $D' = 1$)

[d] Age at onset reported for rs883841 which is in LD with rs35055419 ($r^2 = 0.996$, $D' = 0.999$)

**Table 4**

Expression quantitative trait loci from genome-wide significant associations with CSF levels

| Analyte | SNP | Tissue/cell type | Gene | Effect size | P | References |
|---------|-----|------------------|------|-------------|---|------------|
| $A\beta_{42}$ | Rs316341[G] | Transformed fibroblasts | SERPINB1 | 0.24 | $1.3 \times 10^{-7}$ | [33] |
| $A\beta_{42}$ | Rs316341[G] | Hippocampus | SERPINB1 | 0.30 | $4.3 \times 10^{-5}$ | [73] |
| $A\beta_{42}$ | Rs316339[A] | Transformed fibroblasts | SERPINB1 | 0.24 | $1.9 \times 10^{-7}$ | [33] |
| $A\beta_{42}$ | Rs316339[A] | Hippocampus | SERPINB1 | 0.30 | $3.9 \times 10^{-5}$ | [73] |
| $A\beta_{42}$ | Rs316339[A] | untreated osteoblasts | SERPINB1 | −0.18 | $7.7 \times 10^{-9}$ | [32] |
| $A\beta_{42}$ | Rs316339[A] | BMP2 treated osteoblasts | SERPINB1 | −0.19 | $5.7 \times 10^{-7}$ | [32] |
| $A\beta_{42}$ | Rs316339[A] | DEX treated osteoblasts | SERPINB1 | −0.19 | $3.8 \times 10^{-9}$ | [32] |
| $A\beta_{42}$ | Rs316339[A] | Whole blood | SERPINB1 | $28.96^{a}$ | $2.2 \times 10^{-184}$ | [79] |
| $ptau_{181}$ | Rs12961169[T] | Frontal cortex | CTDP1 | 0.32 | $3.9 \times 10^{-5}$ | [73] |
| $ptau_{181}$ | Rs12961169[T] | Frontal cortex | NFATC1 | 0.29 | $1.7 \times 10^{-5}$ | [73] |

rs316339[A] = chr6.hg19:g.2838046A > G; rs316339[A] is in high LD with rs316341[G] ($r^2 = 0.993$, $D' = 1$)

*SNP* based on Build 37 of reference genome followed by effect allele; *BMP2* bone morphogenetic protein, *DEX* dexamethasone

$^{a}Z$ score